

UKAEA-CCFE-PR(22)60

Y. Zayachuk, I. Jepu, M. Zlobinski, C. Porosnicu, N. Catarino, E. Pajuste, P. Petersson, L. Dittrich, J. P. Coad, E. Grigore, C. Postolache, E. Alves, G. Kizane, M. Rubel, A. Widdowson

Fuel desorption from JET-ILW materials: Assessment of analytical approach and identification of uncertainty and discrepancy sources

Enquiries about copyright and reproduction should in the first instance be addressed to the UKAEA Publications Officer, Culham Science Centre, Building K1/O/83 Abingdon, Oxfordshire, OX14 3DB, UK. The United Kingdom Atomic Energy Authority is the copyright holder.

The contents of this document and all other UKAEA Preprints, Reports and Conference Papers are available to view online free at scientific-publications.ukaea.uk/

Fuel desorption from JET-ILW materials: Assessment of analytical approach and identification of uncertainty and discrepancy sources

Y. Zayachuk, I. Jepu, M. Zlobinski, C. Porosnicu, N. Catarino, E. Pajuste, P. Petersson, L. Dittrich, J. P. Coad, E. Grigore, C. Postolache, E. Alves, G. Kizane, M. Rubel, A. Widdowson

Fuel desorption from JET-ILW materials: Assessment of analytical approach and identification of uncertainty and discrepancy sources

Y. Zayachuk¹, I. Jecu^{1,2}, M. Zlobinski³, C. Porosnicu², N. Catarino⁴, E. Pajuste⁵, P. Petersson⁶, L. Dittrich⁶, J. P. Coad¹, E. Grigore², C. Postolache⁷, E. Alves⁴, G. Kizane⁵, M. Rubel⁶, A. Widdowson¹

¹*United Kingdom Atomic Energy Authority, Culham Centre for Fusion Energy, Culham Science Centre, Abingdon, OXON, OX14 3DB, United Kingdom*

²*National Institute for Laser, Plasma and Radiation Physics, Măgurele 077125, Romania*

³*Forschungszentrum Jülich GmbH, Institut für Energie- und Klimaforschung – Plasmaphysik, Partner of the Trilateral Euregio Cluster(TEC), 52425 Jülich, Germany*

⁴*IPFN, Instituto Superior Técnico, Universidade de Lisboa, 1049-001, Lisboa, Portugal*

⁵*University of Latvia, Institute of Chemical Physics, Riga LV-1004, Latvia*

⁶*KTH Royal Institute of Technology, Fusion Plasma Physics, 100 44 Stockholm, Sweden*

⁷*National Institute for Physics and Nuclear Engineering, “Horia Hulubei” IFIN HH, Măgurele 077125, Romania*

Abstract

This work was carried out to identify sources of errors, uncertainties and discrepancies in studies of fuel retention in wall components from the JET tokamak using methods based on thermal desorption. The parallel aim was to establish good practices in measurements and to unify procedures in data handling. A comprehensive program designed for deuterium quantification comprised the definition and preparation of two types of materials (samples of JET limiter Be tiles, and deuterium-containing targets produced in laboratory by magnetron-assisted deposition), their pre-characterization, quantitative analyses of the desorption products in four different TDS systems and detailed critical comparison of results. Tritium levels were also determined by several techniques in samples from JET and in tritiated targets manufactured specially for this research program. Facilities available for studies of Be- and tritium-contaminated materials from JET are presented. Apparatus development, future research options and challenges are discussed.

Keywords: *Fuel retention, thermal desorption, dissolution, JET-ILW*

List of Acronyms

Acronym	Meaning
AIMS	Accelerator-based In-situ Material Surveillance
AMS	Accelerator Mass Spectroscopy
ASDEX	Axially Symmetric Divertor Experiment
BIXS	Beta-induced X-ray Spectroscopy
CCFE	Culham Centre for Fusion Energy, Culham, United Kingdom
D	Deuterium (^2H)
ERDA	Elastic Recoil Detection Analysis
FTS	Fast Transfer System
FZJ	Forschungszentrum Jülich, Jülich, Germany
GDOES	Glow Discharge Optical Emission Spectroscopy
HIERDA	Heavy Ion Elastic Recoil Detection Analysis
HiPIMS	High Power Impulse Magnetron Sputtering
IAP	Institute of Atomic Physics, Magurele, Romania
IBA	Ion Beam Analysis
ILW	ITER-Like Wall
IPT	Imaging Plate Technique (Radiography)
IST	Instituto Superior Tecnico, Lisbon, Portugal
IWGL	Inner Wall Guard Limiter
JET	Joint European Torus
JET-C	JET with Carbon wall
JET-ILW	JET with ITER-Like Wall
KTH	Kungliga Tekniska Högskolan Royal Institute of Technology, Sweden
LEIS	Low Energy Ion Scattering
LIAS	Laser-Induced Ablation Spectroscopy
LIBS	Laser-Induced Breakdown Spectroscopy
LID(S)	Laser-Induced Desorption (Spectroscopy)
LSC	Liquid Scintillography Counter
MS	Magnetron Sputtering
NRA	Nuclear Reaction Analysis
QMS	Quadrupole Mass Spectroscopy
RBS	Rutherford Backscattering Spectrometry
PFC	Plasma-Facing Components
PFM	Plasma-Facing Materials
PFS	Plasma-Facing Surface
RH	Remote Handling
SIMS	Secondary Ion Mass Spectroscopy
T	Tritium (^3H)
TEXTOR	Tokamak EXperiment for Technology Oriented Research
TFTR	Tokamak Fusion Test Reactor
TDS	Thermal Desorption Spectroscopy
ToF-ERDA	Time-of-Flight ERDA
UoL	University of Latvia
UU	Uppsala University, Sweden

1. Introduction

Fuel retention studies in controlled fusion devices provide basis for the assessment of fuel balance and tritium inventory in current machines, and for predictions of the inventory resulting from the deuterium-tritium (D-T) operation in a future reactor [Federici2001][Counsell2][Loarte2007]. Regular determination of gas balance and deuterium content in plasma-facing components (PFC) was carried in the past in ASDEX Upgrade [Rohde2001][Whyte1999], TEXTOR [Rubel1989][Mayer2001][Rubel2001], TFTR [Skinner1977][Mueller1977] and JET [Coad1989][Coad1989][Coad1997][Coad2001][Andrew1999][Coad2018] tokamaks. The full extent of the issues posed by tritium accumulation was realized after the TFTR [Skinner1977][Mueller1977] and JET [Coad2001][Andrew1999][Coad2018][Penzhorn2001][Rubel2003] operations with a 1:1 D-T mixture: long-term in-vessel retention reaching 35% of the gas input [Andrew1999]. This in turn accelerated both retention studies and work towards the development of fuel control and removal methods [Counsell2]. The latter did not bring promising results in carbon-wall devices [Rubel2012]. The breakthrough in the reduction of fuel retention came with the major change of wall materials in JET: the transition from the carbon wall (JET-C) to the ITER-Like Wall (JET-ILW) with W in the divertor and Be on the main chamber wall [Matthews2007][Matthews2011]. This strong reduction of the carbon source led to the decrease of fuel retention by a factor of 10-20 in comparison to the situation in JET-C [Matthews2013][Loarer2013][Brezinsek2013].

Fuel measurements in plasma-facing components (PFC) fall into two major categories, summarized in Table 1: without breaking vacuum (in the following called “in-situ”) and after venting the torus and retrieval of wall components for analysis in the lab (“ex-situ”). Studies inside the vented machine during shut-downs will not be addressed here. This approach is not practiced in JET at present, because it would require analytical systems integrated with the remote handling (RH) equipment for operations in the Be- and tritium-contaminated environment.

The category of in-situ methods comprises optical spectroscopy [Mass1999][Hillis1997] and gas-balance assessment [Mayer2001][Loarer2007][Tsitrone2011][Pegourie2013], while tritium accountancy in the D-T operation is also based on radiometric, chromatographic and calorimetric measurements [Lasser1999][Lasser1999-2]. This category may be complemented by laser-induced desorption (LIDS), breakdown (LIBS) or ablation (LIAS) spectroscopy techniques [Summers2001][Huber2001][Schweer2007][Philipps2013][Malaquias2013][Zlobinski2020], but to date rather limited number of in-situ measurements of local character have been performed, including also one experiment in JET-C [Summers2001]. Ex-situ analyses are carried out using a large number of tools employing various means for fuel thermal release, a range of IBA techniques and a set of methods for determination of tritium content. Their major features, advantages and drawbacks are summarized in Table 1. Many of those methods have been used for fuel studies in JET materials. However, some of the existing techniques, e.g. in-situ IBA [Hartwig2015], cannot be applied at JET because of the machine size and radioactive environment.

Despite broad research programs and a range of analytical tools used in retention studies, at least two issues in the assessment of retention remain unresolved. These are the discrepancies between: (i) the global gas balance and the assessment based on results of post exposure measurements on PFCs retrieved from tokamaks where the difference by a factor of up to two was reported on several occasions [Mayer2001][Loarer2007][Tsitrone2011][Pegourie2013]; (ii) results obtained by thermal desorption spectroscopy (TDS) in different laboratories when analyzing apparently the same type of wall materials (e.g. wall tiles) retrieved from a given tokamak.

The reported differences by a factor of up to two between the deuterium balance and ex-situ analyses [Mayer2001][Loarer2007][Tsitrone2011][Pegourie2013] may be attributed to (i) an immediate release and/or H-D isotope exchange upon PFC exposure to ambient atmosphere and (ii) inaccuracy in the extrapolation of local surface measurements to the whole machine. Fast processes of D release or H-D isotope exchange are difficult to study using wall probes, because the shortest interval between the probe exposure and D analysis amounts to several hours, i.e. time necessary for the probe withdrawal, venting of the probe system, retrieval of material and transfer to the surface analysis station. The D content measured after such “transfer” time is fairly stable: the decrease of the retained D is of up to 25% over 5 years from that initially determined value [Rubel2007]. It should be stressed that such measurements were possible only in medium size machines, e.g. TEXTOR [Rubel2007], operated with relatively easy access to the probe systems. No studies of that kind were performed in JET, though a Fast Transfer System (FTS) for surface probes was originally constructed [Rebut1985]. It facilitated the transfer in vacuum of the exposed probe from the torus to a surface analysis station but the operation was complex and the system was used only on a very few occasions [Rubel1989][Coad1991] and due to conflicting changes to the furniture within the JET vessel was dismantled in the early 1990s. In practice, the time between the end of plasma operation in JET (start of shutdown) and surface measurements is at least 3-4 months. Secondly, the global balance data are based on daily or long-term fuel accountancy (injected *versus* pumped-out amount) in the whole machine, while surface analyses can be carried out only for a limited number of wall tiles available for retrieval and ex-situ studies. Even the best-planned tile selection does not provide full poloidal and toroidal coverage. This in turn may lead to the inaccurate assessment of total inventory, because the extrapolation is done under the assumption of toroidal symmetry of the erosion-deposition patterns.

The second category of discrepancies or difficulties in TDS studies arises from significant local variations of fuel retention in PFC, in extreme cases also on a micro-scale because of the imperfections in surface topography or tile alignment [Petersson2011][Petersson2012][Bykov2015]. As a consequence, TDS from the adjacent areas, even located only a few mm apart and of apparently identical appearance often yields very different results – while the repetition of destructive TDS measurements on the same sample but under different conditions or in another laboratory is of course impossible. The approach based on the comparison between results of IBA and TDS may be reliable if a very detailed pre-characterization of materials by IBA had been performed beforehand. All such aspects are taken into account in the work presented below.

This work is focused on the comparison and critical assessment of thermal desorption data obtained at various laboratories studying JET samples and lab-produced reference samples manufactured specially for this research program. The overall aim was to improve quantification and further develop good practices in the characterization of PFC in order to improve reliability (consistency) in predictions of fuel inventory in a reactor-class machine, such as ITER. For that reason, and in the view of the ongoing D-T operation in JET [Gibney2022] tritium analysis methods are also discussed although the quantities of that isotope in JET-ILW materials from the three initial ILW campaigns are on a low level not exceeding 1 MBq (or $\sim 5.5 \cdot 10^{14}$ T atoms) per analyzed sample of 0.1-0.3 cm³.

The paper provides an overview of experimental procedures and possible sources of errors and/or discrepancy. The experimental approach is presented, describing selection, preparation, and pre-characterization of JET materials and laboratory-produced reference samples. Analytical capabilities of several laboratories participating in this study are presented. A comprehensive section with results for deuterium and tritium retention is concluded with recommendations regarding procedures in analyses and selection of reference materials.

2. Experiment

The pre-requisite for comparative studies of deuterium and tritium retention is the availability of specimens with as-close-as-possible contents of a species to be quantified upon thermal release. Several types of samples of this kind were selected and manufactured: (a) pieces of the castellated bulk Be limiters (retrieved from JET); (b) Mo plates coated with a magnetron-deposited layer of W co-deposited with either H or D (lab-produced); (c) Mo plates coated with a layer of T-saturated W (lab-produced). Measurements included TDS, IBA and the dissolution method (only for T). Details are given in the following sub-sections.

2.1. Samples retrieved from JET – beryllium limiters

Fuel retention in all types of PFCs retrieved from JET was examined with IBA and TDS in the past [Likonen2019][Baron2015][Petersson2015][Heinola2016][Heinola2017][Heinola2017-2][Widdowson2017][Widdowson2017-2][Widdowson2020][Krat2020][Mayer2016][Rubel2017][Rubel2016][Rubel2020][Catarino2017].

Based on the obtained knowledge of the erosion-deposition and fuel retention patterns, the decision was made regarding the sample selection and preparation. Samples were produced from the Be tiles of an outer wide poloidal limiter (WPL, tile 4D14) and an inner wall guard limiter (IWGL, tile 2XR10), retrieved during the shut-down following the third ILW campaign [Widdowson2020]. Fig. 1 shows the images of the selected tiles and their corresponding locations within the poloidal cross-section of the JET vessel.

Individual 12x12x12 mm castellations were cut from several positions across the tiles (marked by crosses and identification numbers in the Fig. 1); these positions cover the entire toroidal width of a tile and thus the selected castellations capture erosion and deposition zones, representing different mechanisms of fuel retention. Afterwards, each castellation was further cut into a set of four so-called “quarter samples” (sized 5.5x5.5x1.5 mm), labelled A to D. All cutting was done at the Institute of Atomic Physics (IAP), Romania, using procedures described

in [Rubel2017]. Afterwards, the deuterium contents in the surface layers of respective pieces were determined by means of IBA (NRA and RBS), using a 2.5 MeV $^3\text{He}^+$ beam at the Instituto Superior Técnico (IST), Portugal. Following this, samples were distributed to four participating laboratories: 1) IAP (referred to in the following discussion as Facility A), 2) CCFE (referred to as Facility B), 3) University of Latvia (UoL; Facility C) and 4) Forschungszentrum Juelich (FZJ; Facility D), for TDS (IAP, CCFE and FZJ) and dissolution (UoL) measurements.

2.2. Laboratory-produced samples – tungsten-coated molybdenum

These samples, referred to as the “reference samples”, were produced at IAP using High Power Impulse Magnetron Sputtering (HiPIMS). A nominally 2 μm thick W layer with D was deposited on a polished Mo substrate with the dimensions of 12x12x1 mm. All samples were manufactured in a single run to maximize sample uniformity. Two samples were sent to each of the three participating laboratories (IAP, CCFE and FZJ) for TDS measurements; these were performed on the same day in each participating lab to ensure that the discrepancy in measured contents due to a difference in a time delay between manufacturing and measurement was eliminated. In parallel, two other sets of samples were analysed by ion beam methods to determine the gas content and sample purity; see Section 2.5.

2.3. Laboratory-produced samples – tritiated tungsten-coated molybdenum

Laboratory-produced tritiated W-coated Mo samples are referred to as “tritiated samples”. A set of samples that were 2 μm W coated on Mo plate obtained as described in the previous section but not having any gas inclusions were placed in a Pyrex glass tube using spacers consisting of glass rings 10 mm in diameter and 5 mm thick and quartz wool (see Fig. 2a). The glass ampule with W coated Mo samples was placed inside of a tubular furnace RT 50-250/11 with Nabertherm-type temperature controller and connected at a tritium manifold with vacuum facility (see Fig. 2b).

The glass ampule with W-Mo samples was preliminary vacuumed at room temperature (1 h at pressure below 1 Pa) and degassing at 1273 K (1 h at pressure below 1.3×10^{-2} Pa). The W-Mo samples were put in contact with $\text{T}_2\text{:}^3\text{He}$ mixture extracted from an old tritium gas source [Matei2008]. The samples were kept in the $\text{T}_2\text{:}^3\text{He}$ atmosphere for 196 hours at 200°C, followed by slow decrease of the temperature to the room value and maintaining at this temperature for minimum 8 hours. The residual $\text{T}_2\text{:}^3\text{He}$ was transferred in the glass ampule using a Toepler pump and the tritium trace removed using a high vacuum pump.

The activity of the tritiated W-Mo samples was determined by total combustion method [Raty2019]. Two samples were analysed using a total combustion/calcination facility. The total combustion/calcination facility consist of (a) Oxygen supply, (b) Tandem tubular furnace, first for combustion/calcination of samples and secondary for catalytic oxidation of the flue gases, (c) Tritiated water collector on the bubbling principle, with four retention vials. The total combustion protocol was the following:

- Oven / CuO catalytic bed temperature: 800°C
- Oven / Incineration of samples temperature: 1000°C

- Oxygen flow rate: 4 l / min
- Combustion boat made of Cu.
- In the combustion boat were added 2 g of anhydrous sodium carbonate for retention of Molybdenic Anhydride vapours generated in the calcination step.
- HTO retention: Fresh distillate water (4 vials with 5 ml each).
- HTO activity from the retention vials determination by 1 ml sampling in 16 ml ULTIMA-GOLD M Liquid Scintillator and activity measured at LSC TRICARB TR2800 Perkin Elmer type.
- The oxidation and HTO retention yield was determined: using sample controlled contaminated with Testosterone-1,2-T. The obtained value was 94 + 3% [Fugaru2020].
The mean activity on the two samples was determined to be 160 + 2.895 MBq.

2.4. Thermal desorption measurements

Thermal desorption spectroscopy measurements were performed at all four participating laboratories. Samples measured in each have the corresponding index, e.g. 463A for a sample measured at Facility A.

- IAP (Facility A; reference [Dinca2021]): the heating system of this instrument is an oven, with samples being placed in the quartz tube; it provides a programmable heating rate up to 15 K/min, with the maximum temperature of 1323 K. Temperature control is provided by a type K thermocouple placed inside the oven; the actual temperature on the sample is deduced based on calibration (sample temperature as a function of oven temperature). Gas analysis is performed with a quadrupole mass spectrometer. Be and T-containing samples can be analyzed.
- CCFE (Facility B; reference [Baron2018]): the heating system is a molybdenum heating plate, with samples placed on it; heating rate up to 30 K/s, with the maximum temperature of 1273 K. Temperature control is provided by a type K thermocouple attached to the heater such that the temperature of the heater is measured and recorded. Gas analysis is performed with a line of sight quadrupole mass spectrometer. Be and T-containing samples can be analyzed. Special measures are taken when Be samples are measured: (1) maximum temperature is limited to 1050 K because at higher temperatures Be evaporation occurs (which is undesirable and needs to be avoided because it leads to the contamination of the detector, vacuum chamber and its windows); (2) a protective layer of AlN is placed between sample and heater to avoid adhesion of the sample to the heater at elevated temperature.
- FZJ (Facility D; reference [Zlobinski2019]): the heating system of this instrument is an oven, with samples being placed in the quartz tube, similarly to facility A. Heating rates of up to 100 K/min are possible, with a maximum temperature of 1433 K. Gas analysis is performed with two quadrupole mass spectrometers simultaneously, capable of discriminating D₂ and He. The temperature for the heating control is measured with a type K thermocouple inside the quartz tube. Be and T-containing samples can be analyzed. Be samples are covered by a smaller, exchangeable quartz half-tube that provides a large exit for the desorbed gases through a quartz labyrinth which hinders evaporating Be from contaminating the main quartz tube.

To unify the conditions of thermal treatment and then to make the inter-laboratory comparisons possible, identical heating scenarios were applied in all participating TDS facilities for the quarter and reference samples, as follows:

- Quarter samples – heating rate 10 K/min, maximum temperature 1050 K, hold time at maximum temperature 1 hr. Signals of masses 3 (HD molecules), 4 (D₂ and HT), 5 (DT), 6 (T₂) were monitored to quantify released amounts of D and T. Atomic D release flux F_D was calculated as a sum

$$F_D = F_{HD} + 2F_{D_2} \quad (\text{Equation 1})$$

where F_{HD} and F_{D₂} are molecular release fluxes of masses 3 and 4, respectively. Atomic T release flux F_T was calculated as a sum

$$F_T = F_{DT} + 2F_{T_2} \quad (\text{Equation 2})$$

where F_{DT} and F_{T₂} are molecular release fluxes of masses 5 and 6, respectively. In addition, signals of masses 18 (H₂O) and 20 (D₂O and HTO) were recorded.

- Reference samples – heating rate 10 K/min, maximum temperature 1275 K, hold time at maximum temperature 1 hr. Signals of masses 3 and 4 (HD and D₂) were monitored to quantify released amounts D, using Equation 2. In addition, signals of masses 18 (H₂O), 19 (HDO) and 20 (D₂O and HTO) were recorded.
- Tritiated sample – heating rate 10 K/min, maximum temperature 1275 K, hold time at maximum temperature 1 hr. Signals of masses 4 (HT molecules) and 6 (T₂) were monitored to quantify released amounts of T. Atomic T release flux F_T was in the case of these samples calculated as

$$F_T = F_{HT} + 2F_{T_2} \quad (\text{Equation 3})$$

where F_{HT} and F_{T₂} are molecular release fluxes of masses 4 and 6, respectively. In addition, signals of masses 18 (H₂O), 19 (HDO), 20 (D₂O and HTO), 21 (DTO) and 22 (T₂O) were recorded.

In all facilities quantification of measured release signals was performed using calibrated leaks. H₂ calibrated leak was used for determination of calibration factor for mass 2 release signal, D₂ calibrated leak was used for calibration factor for mass 4 release signal in case of D-containing samples, He leak was used instead for calibration factor for mass 4 release signal in case of He-containing samples. Calibration factor of mass 3 (HD molecules) was calculated as an average of factors for masses 3 (H₂) and 4 (D₂). Factors for masses 5 and 6 (DT and T₂ molecules) were calculated by linear extrapolation of factors for masses 2 (H₂) and 4 (D₂). Other signals were not quantified.

2.5. Ion beam analysis measurements

Ion beam analysis was performed at IST and at the Uppsala University (UU), Sweden.

At IST D retention was measured using the 2.5 MV Van de Graaff accelerator at Laboratory of Accelerators and Radiation Technologies (reference [Catarino2020]). The accelerator is equipped with a chamber dedicated to fusion research, where Be- and tritium-containing samples are handled. Rutherford backscattering (RBS) and nuclear reaction analysis (NRA) were performed using ^3He ions at an energy of 2.3 MeV, in order to measure the amounts of D in the investigated Be samples; NRA of W and Be samples was based on proton and alpha-particle detection from $\text{D}(^3\text{He},\text{p})^4\text{He}$. All $\frac{1}{4}$ Be samples were measured before TDS analysis and a selection measured after TDS.

At UU measurements were performed at the Tandem Laboratory located at the Ångström Laboratory of UU. The laboratory has capabilities for handling radioactive and contaminated materials. A 5 MeV National Electrostatics Pelletron was used to examine W-coated samples with the time-of-flight heavy ion elastic recoil detection analysis (ToF-HIERDA with a gas ionization chamber [Strom2016]) using a 36 MeV $^{127}\text{I}^{8+}$ beam and NRA with a 4.5 MeV $^3\text{He}^+$ beam. ToF-HIERDA allowed for the detailed quantitative determination of surface composition and depth profiling of H to W (up to the depth of 2000×10^{15} atoms cm^{-2}), while the total amount of D in the W-coated samples was accomplished with NRA.

2.6. Dissolution tritium measurements

Dissolution measurements were performed at the University of Latvia (Facility C). Details of the experimental setup can be found in [Pajuste2019]. In this technique, investigated samples are etched – chemically (Be samples, using sulphuric acid) or electrochemically (W samples, using 30% KOH solution) – such that tritium is released simultaneously with the dissolution of the sample. Tritium is released in molecular and atomic forms as part of different chemical compounds in liquid and gas phase; its amount is determined radiometrically, with the activity measured in the liquid phase by LSC and in the gas phase by a proportional counter and tritium monitor TEM 2102A, Mab Solutions GmbH.

3. Results

3.1. Quarter samples

Quarter samples were first characterized using IBA. Fig. 3 presents the comparison of D retention values obtained by IBA on quarter samples, superimposed with IBA data taken across the whole tile prior to cutting. Measurements on quarter samples compare well with the results of whole-tile scans, capturing the distribution of D across the tile as well as actual values of D retention. At the same time, they demonstrate that there is a difference in measured D contents between the quarters within the same set, even though they are originating from the same castellation. The difference in D retention between the individual quarters (within a set) ranges between factors of 1.3 and 2.4, with a factor of difference, averaged over all sample sets, being ~ 1.5 (or 50%).

Comparison of the total D retention for TDS measurements at different facilities, plotted as a function of position within their tile of origin, is presented in Fig. 4. It can be seen that the values of retention obtained at different facilities are comparable, with the average difference between the quarters within the same set being ~250%. Results of TDS in Fig. 4 are superimposed with the results of IBA scan of the corresponding tiles, demonstrating that the overall distribution of D across the tile is similar as measured by both techniques, with higher D retention in the wings (deposition-dominated zone) and lower in the center (which is erosion-dominated). The overall tendency is for TDS to show somewhat higher values of retention compared to IBA; this is particularly pronounced in the central region of a tile.

Fig. 5 presents an example of the comparison of the spectra produced in different TDS facilities; normalized spectra are shown here to emphasize the shapes of the peaks. It is evident that all instruments capture the same fundamental shape of the spectrum, featuring a single well-defined release peak (it should be noted that shapes of the spectra of the samples originating from different parts of the original tile are different; some sets of quarters feature multiple release peaks). However, while the exact positions of release maxima obtained at the facilities A and D are essentially identical, the position of the peak of spectrum B is shifted towards higher temperature by ~ 40 K. Similar behavior is observed in all investigated sets of quarter samples. This shift in peak position is not a universal constant – for different sets of quarters it varies and generally lies in the range of ~0-150 K. Moreover, it can be seen that it is not a constant offset – temperature shift increases with the increase of nominal temperature (presented by the arrows in the example in Fig. 5). The reason for this discrepancy will be explored in Section 4.3.

Several selected samples underwent IBA measurements before and after TDS measurements were performed on them. Fig. 6 presents the remaining amount of D in samples as a fraction relative to the initial amount measured prior to TDS (as percentages). It is evident that after a regular TDS run to a maximum temperature of 1050 K, a measurable fraction of deuterium remains unreleased, up to ~30% in some cases. As two of the TDS facilities used, A and D, are capable of a maximum temperature of 1275 K, two sets of quarters were selected (specifically castellations 460 and 524), where the maximum temperature was different for the different samples: one sample was heated to 1050 K in facility B and two to 1275 K in facilities A and D. Fig. 6 presents the comparison between the results, and it can be seen that heating to 1275 K significantly reduces the remaining fraction, by a factor of 5 to 15, bringing the unreleased fraction of D to less than 3%.

Fig. 7 presents the comparison of the tritium contents obtained from across the IWGL tile at TDS facilities B and D, and at dissolution facility C. The difference between the TDS instruments is significant – close to two orders in magnitude in certain locations. At the same time dissolution results are considerably lower than those of both TDS facilities, by up to almost three orders of magnitude.

3.2. Reference samples

Composition of the surface region of the tungsten coatings of the reference samples, including impurity contents, measured using ToF-ERDA method at UU are presented in Table 2.

Comparison of the values of D retention in the reference samples, measured by IBA and TDS, is presented in Table 3. Overall, the IBA results differ within ~20%; TDS results are identical within ~40%. In addition, in the facility B two samples from the set were measured, and the results for these two samples are very similar (less than 5% difference).

Comparison of the spectra produced in the three TDS facilities (Fig. 8, normalized spectra are presented) shows a specific trend. While all the spectra have similar overall shapes, the spectra produced in the facilities A and D have essentially identical positions of release peaks. At the same time, results of B show the tendency to shift towards higher temperature, with the magnitude of this shift increasing with temperature, similarly to that observed in quarter samples (section 3.1).

3.3. Tritiated reference samples

Comparison of the values of T retention in the tritiated samples, measured by TDS (in Facilities A and B; due to technical issues measurements in Facility D could not have been performed) and dissolution (Facility C), is presented in Table 4. Overall the results vary by ~220%. The difference between the results of dissolution and TDS in facility B is within ~36%. At the same time, the difference between dissolution and TDS in facility A is larger, ~140%.

Fig. 9 presents the comparison between normalized spectra of atomic tritium release measured in facilities A and B. It is evident that the overall shapes of spectra are similar, with peaks at ~800 K and 1020 K, with the low-temperature peak being dominant. Positions of the peaks do not coincide exactly. The difference in the position of the low-temperature peak is ~35 K (835 K in A, 800 K in B); the difference in the position of the high-temperature peak is ~40 K (975 K in B, 1015 K in A)..

4. Discussion

4.1. Measurements of deuterium retention

From the perspective of the main topic of this work – determination of how comparable the results of different TDS facilities are – the main observation of the work is that the results of TDS measurements on similar samples are well comparable. The difference in measured values of total retention is ~40 % for highly reproducible reference samples. IBA was performed on each of the investigated samples as a way of independent verification of how similar they were in terms of D retention. IBA on two of the reference samples yielded the values of $7.4 \cdot 10^{17}$ and $8.8 \cdot 10^{17}$ D/cm² (a difference of ~20%). This value can be considered a measure of the inherent difference between the reference samples due to manufacturing uncertainties, and hence the lower bound for the possible difference in D retention values measured by TDS. On

the other hand, for these samples the results of TDS deviated up to ~40% between the labs. The fact that TDS results discrepancy is larger than that of IBA results suggests that the observed difference has a contribution from non-inherent discrepancies – i.e., pertaining specifically to TDS measurements. Notably, this TDS-specific discrepancy – the difference between total TDS and IBA discrepancies – is small, only ~20%. This is an encouraging result, indicating that in general, similar samples do indeed yield similar results.

In case of JET samples the average difference between Be quarter samples within the same set is somewhat higher, ~250%. On the other hand, the average difference between the results of IBA within a set of quarters was ~150%, which indicates that for these samples the TDS-specific discrepancy is larger, ~100%.

The TDS-specific discrepancies (which determine both the difference between measurements at different facilities, and between TDS and IBA) are attributed to the following sources:

(Factor 1) Incomplete desorption leading to uncertainty in D quantification;

(Factor 2) Inherent difference between IBA and TDS techniques due to difference sampling depths/volumes and sensitivity to inhomogeneities from quarter samples;

(Factor 3) Uncertainty of the QMS calibration;

(Factor 4) Unquantified fraction of D released in HDO and D₂O molecules.

In the following discussion these factors will be analyzed and referred to using the numbers from this list.

(Factor 1): From Fig. 6 it is evident that not all D is released from the Be quarter samples during a regular TDS run to the maximum temperature of 1050 K (and even when the maximum temperature is 1275 K, though to a much lesser extent), and therefore it can be concluded that TDS measurements on Be samples will underestimate the true values of D content present (leading to the factor (1)). However, this underestimation is relatively minor – the fraction of D that is undetected in TDS is ~30 % even in worst cases, and usually less than 20%. It should be noted that there is a significant scatter between the remaining fractions from sample to sample – the remaining D fraction ranges between ~2 and 30 % (Fig. 6). Comparison of the release spectra from the corresponding samples (Fig. 10) demonstrates that this difference in remaining D fraction originates from the difference in the position of release maximum in the corresponding desorption spectrum. Samples with a large remaining fraction (such as 463B in the example in Fig. 10) are the ones where the maximum of release is at higher temperature (in case of 463B at 970 K), close to the maximum temperature of the TDS run (1050 K). As a consequence, at the beginning of the holding period the release rate is still high (comparable to that at the maximum), and hence by the end of the holding period, during which release rate progressively decreases, release rate is still substantial, reflecting a significant remaining amount of D. In contrast, for the samples with the maximum of release at lower temperatures (example of 569B in Fig. 10, at 880K), the hold time is more effective at removing the remaining D, with release rate falling to near-background levels by the end of its duration. Therefore it can be expected that TDS results from Be samples where the maximum of release is shifted to higher temperatures (in particular close to the maximum temperature of the run) will tend to have a higher degree of underestimation.

In light of this it can be suggested that a preferable procedure for TDS measurements on Be samples is heating them up to the highest temperature available for the equipment, which in

this case is a maximum temperature of 1275 K for Facilities A and D. However, when this is not possible, the degree of underestimation is on the order of few tens of percents.

(Factor 2): The ratio of D retention values measured by IBA to those of TDS on the same individual quarters is plotted as a function of position within a tile in Fig. 11, where the results from all facilities are summarized. Comparison between TDS and IBA results demonstrates that TDS tends to systematically yield higher values of D retention compared to IBA. This can be attributed to the fact that detection ranges (i.e., the depth of retained D that is detected) are different, with IBA only probing near-surface region ($\sim 5 \mu\text{m}$ in the conditions implemented in this study), whereas TDS detects D coming from the entire sample volume, including the bulk region beyond the IBA detection range. Therefore, when comparing TDS and IBA an additional source of discrepancy due to this difference in probed ranges (factor (2) in the list above) arises.

It is also evident that there is a certain spatial distribution of the difference between IBA and TDS. In the center of a tile D IBA-to-TDS ratio of retention is low and tends to increase towards the periphery. This indicates that in the center – which is an erosion-dominated zone – the majority of D is retained in the bulk, outside of the first $5 \mu\text{m}$ from the surface, and is therefore governed by diffusion and trapping. At the same time, at the periphery – a deposition-dominated zone – the majority of trapping occurs within the co-deposits and the majority of the D is therefore located close to the surface, accessible to IBA probing.

It should be noted that it is unphysical to have higher total retention measured by IBA than TDS, since by definition IBA only measures a fraction of the volume measured by TDS, thus IBA-to-TDS ratio should never exceed 1. It can be seen, however that in some cases, all of which are located at the periphery of the tiles (within deposition-dominated zone), this ratio is higher than 1. This reflects the fact that the size of the ion beam spot is $\sim 1 \text{ mm}^2$, i.e., it is smaller than the dimensions of a quarter sample. Therefore IBA results here are more sensitive to the local inhomogeneity of D content (such as individual D-rich co-deposit particulates, for example, which can be present within the beam spot leading to the increase of observed D content, but not reflecting true overall D content within the sample). Incidentally, this local inhomogeneity is a contribution to the observed variation in IBA results themselves noted in the Fig. 3. Additionally factor 1 (incomplete D release) also contributes to IBA-to-TDS ratio exceeding 1 as an underestimation of the total retention drives the IBA-to-TDS ratio up.

(Factors 3 and 4): Uncertainty in calibration and in unaccounted contribution of other D-containing molecules can be addressed by using the results from the reference samples, which, since they are lab-produced, are inherently more comparable. Importantly, factors (1) and (2) from the list above are not relevant for the reference samples. W-coated Mo samples were heated to 1275 K, and, as is evident from Fig. 8, D release ceases by the time the maximum temperature is reached, which means that no unreleased D remains unaccounted for in the sample following the TDS measurement. Hence one expects no discrepancy due to factor (1). Since the deuterium-saturated W layer is $\sim 2 \mu\text{m}$ thick, the IBA probing depth covers the entirety of it, and thus the probed depth region is the same for IBA and TDS, eliminating the influence of the factor (2) as well.

It was noted above that TDS-specific difference in D quantification between reference samples is $\sim 20\%$. Given the arguments above, this can be considered as an estimate of the combined contributions of factors (3) and (4) to the discrepancy arising between TDS instruments. Deconvolution of these factors is not possible due to the difficulty in calibrating

HDO and D₂O contributions, but these are very likely different between the systems. This conclusion stems from the fact that the relative contributions of HD and D₂ molecules is different between the instruments (percentage of D released in the form of HD molecules is ~17% in facility B, ~19% in D, but ~30% in A), possibly due to different background levels of residual H₂ and in particular H₂O in the vacuum chambers, and it is therefore reasonable to assume the kinetics of formation of other molecular species are also different. However, since the results of TDS instruments are generally similar in total D quantification and desorption characteristics, and also similar to IBA results, it can be concluded that contributions of unquantified D-containing molecular species (factor (4)) is small; correspondingly, contribution of factor (3) must be small as well.

Based on these findings it can be concluded that, barring severe experimental errors such as incorrectly determined calibration factors, values of retention reported from different laboratories are comparable for practical purposes. Especially for highly reproducible lab-produced samples the discrepancy between the systems is only ~20%. Technical solutions such as improved determination of calibration factors for deuterium-containing molecules, and improvement of vacuum in the measurement chamber (with the associated decrease of H₂ and H₂O backgrounds) can be recommended to improve the degree of measurement precision and therefore comparability.

4.2. Measurements of tritium retention

The data plotted in Fig. 3 shows a large discrepancy (close to 3 orders of magnitude for some sets) in the T quantification of the quarter samples, both between different TDS instruments, and between TDS and dissolution. However, on examining the mass 5 (DT) and 6 (T₂) spectra it is evident that these signals are essentially at the level of noise, see figure 12, and therefore T quantification using QMS signals of DT and T₂ molecules at these low concentrations is not possible. The intrinsic noise level will be governed by pumping and vacuum conditions for individual systems.

This could be expected since presently only trace amounts of T are present in ILW JET tiles. This is due to the fact that between the installation of ILW and extraction of the tiles used for the measurements following ILW3 campaign, only H and D were used in JET, and thus all T present is coming either from implantation of energetic T produced in the D-D reaction, or neutron-induced transmutation of Be, in addition to residual inventory from the previous D-T campaign in 1997 (pre-ILW) [Pajuste2021].

On the other hand, T contents obtained in dissolution measurements are not resulting from QMS-based detection of molecular species, but on the direct measurements of radioactivity of released tritium. This activity can be accurately measured even at very low T concentrations, and in addition these measurements are not affected by the molecular state of T. Therefore, it can be concluded that at the current tritium levels in Be tiles of JET ILW— namely, on the order of 10¹² at/cm², measurements of QMS-based TDS do not allow reliable quantification of tritium content and distribution. In contrast to these, the radiometry-based dissolution method, where activity of released tritium is measured, as opposed to detection of molecules by QMS, is much more sensitive to low concentrations of tritium and is therefore preferable for analysis of tritium distribution in JET tiles at the present tritium concentrations.

Lab-produced tritiated samples contained considerably higher amounts of tritium, $\sim 10^{16}$ at/cm². Indeed, it can be seen that at this tritium content results of TDS and dissolution are comparable (Table 4), indicating that determination of tritium content in QMS-based instruments becomes feasible when it is sufficiently high. The exact tritium content where this transition occurs has not been established. However, considering both the results from quarters and tritiated samples, an estimate can be suggested. As per Fig. 12, for QMS-based TDS the signal of tritium-containing molecules at essentially noise level results in the calculated tritium contents of $10^{12} - 10^{14}$ at/cm², even when radiometrically-measured contents are much lower. This suggests that any concentration of tritium below these levels would be lost in noise and is therefore not measurable by QMS-based TDS. Thus, the transition to a content where this measurement becomes possible by this technique lies in the $10^{14} - 10^{16}$ at/cm².

Despite the low concentration of T in the quarter samples presented here, it is important to note that in the 2021 DTE2 campaign in JET 50-50% D-T mixture has been used, indicating that following this campaign the amounts of tritium retained in the PFC will be comparable to that of deuterium. Consequently, based on the results of tritiated reference samples, where the amounts of T are comparable to those of D in typical JET samples and are reasonably confidently quantified using QMS-based TDS measurements, it can be expected that when in the future PFCs are extracted from JET (i.e., following the DTE2 campaign), quantitative studies of T retention using TDS will be possible. Of course, the same holds true for eventual studies of PFCs extracted from ITER.

4.3. Desorption spectra

Comparison of the desorption release spectra produced at different facilities demonstrates that overall shapes of the spectra are captured by all of them. However, a systematic difference was observed in terms of the positions of the release peaks. While facilities A and D produce spectra with peaks at essentially identical temperatures, spectra from B are systematically shifted towards higher temperature. Moreover, as noted in sections 3.1 and 3.2, this shift is not a constant offset – the higher the temperature, the larger the shift.

To explain this behavior one should note that, as mentioned in the experimental description, facilities A and D are using the same type of heating system, while the heating system of B is different. In A and D, a sample is placed inside a quartz tube and heated within an oven; in contrast, facility B has a sample placed onto a heating plate, with a protective AlN layer between the heater and the sample. It should be emphasized that the protective layer is necessary for use with Be samples to avoid bonding the sample to the stage as a result of localized heating; and while in case of W-coated Mo reference samples it is technically not necessary, it was still used to keep experimental conditions the same for comparison purposes. Therefore, it can be suggested that the difference in the way heating is applied leads to the observed changes in release temperatures.

The fact that there is no need to use AlN layer with the reference W-coated Mo samples was utilized to study the effect of AlN on the spectral shapes and peak positions in facility B. Two reference samples were measured, one with and one without an AlN layer. Comparison of the corresponding spectra is shown in Fig. 13, and it is evident that indeed the presence of AlN layer modifies the spectrum in the same way as observed above – positions of peaks shift

towards higher temperature, and this shift increases with temperature. On the other hand, from Fig. 13 it is also evident that the peak positions produced without AlN in facility B are close to those produced in facility D, i.e., in the absence of AlN the abovementioned systematic temperature discrepancy disappears.

This behavior can be explained as follows. Because of the additional step of thermal transfer through the AlN layer, as well as through the AlN-heater interface, the true temperature of the sample surface is lower than the nominal temperature measured at the heater, and this temperature delay between the heater and the sample increases with the increase of heater temperature. In the spectra produced by B, the sample temperature (not measured directly) is considered to be equal to the heater temperature (which is the one that is measured and recorded). But because of this delay, in the presence of the AlN layer this assumption does not hold, and the true temperature of the sample is lower than assumed.

Comparing the positions of the characteristic points on the spectra measured with and without AlN (in the case of the reference samples), as well as spectra of the quarters measured with AlN on the plate heater in facility B and those without it in the oven in A and D, it is possible to quantify the effect of this heating delay due to the AlN layer. Fig. 14a presents an example of such a procedure for a single spectrum. Arrows indicate the temperature difference created by the AlN layer at different nominal heater temperatures. Note that this assumes that such normalized spectra should be identical in the absence of AlN. Dependence of temperature difference, calculated in such a way, on nominal heater temperature is presented in Fig. 14b. The points in the plot are taken from a number of spectra, both comparing results of W samples with and without AlN measured at facility B, and Be samples measured with AlN at facility B with those measured at other facilities. It is evident that the increase of temperature difference as a function of nominal temperature can be well fitted by a linear dependence with a slope of 0.193. This means that the temperature ramp experienced by the sample is still constant, but it is lower than the nominal value of 10 K/min. Instead it is equal to $10 \cdot (1 - 0.193) \sim 8.1$ K/min.

The value of heating rate at the sample surface can be used in order to perform a re-calibration of temperature measurement and compensate, at least partially, the effect of the temperature delay introduced by the AlN layer. Since the heating rate is still constant, dependence of the sample temperature as a function of time can be calculated, replacing the heating rate at the heater stage, 10 K/min, by the calculated rate of 8.1 K/min. An example of a corrected spectrum produced in this way is shown in Fig. 13, and it is evident that the positions of the peaks in the corrected spectrum become similar both to those produced by the sample measured without AlN, and to those produced by the sample measured at a different facility.

It should be noted that, as seen in Fig. 14b, there is a significant scatter of the values of temperature difference obtained from different samples – the deviation from the calibration line reaches ~ 60 K. This can be considered to be an inherent uncertainty in the determination of sample temperature that cannot be eliminated by a single calibration function. Several factors contribute to this scatter in true surface temperature from sample to sample. Since D is mainly retained in the near-surface region, and the sample is heated from the opposite side on the plate heater, a certain temperature difference is introduced due to thermal transport within the thickness of the sample itself. This difference would depend on the material, and hence be different for W, bulk Be and Be co-deposits (where additional thermal transport step through the deposit-substrate interface will be present), and indeed any other investigated material, but

also on the thickness of the individual sample. In addition, sample-specific uncertainty arises also because different samples would have different shapes and roughness of the back surface, and as a result thermal contact between the surface and the sample will be different for each sample and cannot be quantified in a general way. Therefore, the influence of these different factors would vary from sample to sample, but the figure of ~60 K is a reasonable general estimate of maximum uncertainty.

Since temperature positions of release peaks are used in the modeling of diffusion and trapping in order to determine trapping energies E_T for hydrogen isotopes in materials, the shift in temperature as measured by TDS can potentially influence the obtained values of E_T . In order to estimate to what degree the observed temperature uncertainty translates into the uncertainty in E_T , a simple analysis using the Kissinger method can be applied. In this method, positions of the release peaks are measured at different heating rates and plotted as values of $\ln(\varphi/T_c^2)$ as a function of $1/T_c$, where φ is heating rate and T_c is peak temperature position, known as Choo-Lee plot. The trapping energy E_T is then related to the slope of the linear dependence of

$$\ln(\varphi/T_c^2) \text{ as } \frac{\partial(\varphi/T_c^2)}{\partial(1/T_c)} = -\frac{E_T}{R}, \text{ where } R \text{ is the gas constant.}$$

Assume, as an example, a release peak located at 800 K with heating rate of 10 K/min, corresponding to a trapping energy of 1 eV. Based on the assumed value of E_T the slope of the straight line can be calculated; from there, the intersections of this straight line with the lines corresponding to other heating rates can also be calculated, and hence positions of release peaks that correspond to those heating rates can be determined – in this example, the peak would be located at 768 K at the heating rate of 5 K/s and 835 K at the heating rate of 20 K/s (circles in Fig. 15a). Now each of these peaks is shifted by an assumed value of temperature uncertainty, and correspondingly a new set of points in Choo-Lee plot is formed (triangles in Fig. 15a). A straight line is then fitted to this newly formed set of points, its slope is calculated and a corresponding E_T is determined. In the particular example shown in Fig. 15a, if the peaks shift by 100 K, the original value of 1 eV changes to 1.24 eV (a relative change of 24%).

Using this method, it is possible to calculate the relative uncertainty in E_T corresponding to the uncertainty in temperature measurement of 60 K. This is presented in Fig. 15b as a function of nominal heater temperature (for comparison, relative uncertainties caused by the temperature uncertainty of 30 K and 100 K are presented as well). Alternatively, the plots of relative uncertainty in E_T for different temperature uncertainties can be replotted as function of relative temperature uncertainty, as presented in Fig. 15c. It is evident that for any absolute temperature uncertainty, such a dependence follows the same smooth curve. Notably, this relative change is almost independent of the E_T , with a small decrease at higher trapping energy. It can be seen that in the temperature range where release peaks of Be samples are located, ~800-1000 K, for the temperature uncertainty of 60 K (corresponding to relative uncertainty of 6-7.5 %), the relative uncertainty in trapping energy is ~15%.

In the context of the topic of this paper the main conclusion in regards to shapes of desorption spectra is that TDS facilities with different heating systems might produce spectra with somewhat different positions of the desorption peaks. Plate-type heaters, where samples are pressed to the flat heating surface and are heated from the back while desorption is detected from the front tend to introduce random scatter in the positions of peaks, due to difference in

sample geometry and mounting, as well as introduce a systematic progressive shift of the spectra towards higher temperatures. However, this scatter – the temperature uncertainty – is shown to be in the range of several tens of K, and this translates to a relatively small uncertainty in the determination of trapping energy (~15 % for the temperature range where desorption peaks are located in Be). Therefore it can be concluded that quartz tube-type heating systems seem preferable as they are less susceptible to thermal gradients across the sample and associated uncertainty in sample temperature than the plate-type heating system for these types of samples that are relatively thick.

5. Summary and outlook

A comprehensive research exercise was designed and accomplished to address critical issues in the quantification of fuel inventory in Be- and tritium-contaminated PFC from JET-ILW. In particular, the sources and the magnitudes of the discrepancies between the results obtained at independent TDS instruments, as well as between TDS and other techniques – IBA (in case of measurements of deuterium content) and dissolution (in case of tritium), were studied and quantified.

Insofar as measurements of deuterium contents in JET Be samples are concerned, it was found that the discrepancy between different TDS instruments is close to a factor of ~3.5 (250%). Part of this discrepancy is due to the inherent differences between the investigated samples, which were established to be ~150% by IBA. The main sources of additional – TDS-specific – discrepancy include:

- (1) uncertainty of remaining D contents, not released during the TDS measurement;
- (2) uncertainty of the QMS calibration;
- (3) unquantified fraction of D released in the form of HDO and D₂O molecules.

Uncertainty in remaining content arises from the fact that in some TDS systems the maximum temperature a Be sample can be heated to is limited by the onset of Be evaporation that starts above 1050 K. It was found that at this temperature up to ~30% of D might remain unreleased, leading to a corresponding underestimation of measured retention. This underestimation is correlated with how close the maximum of high-temperature release peak is to the beginning of the maximum temperature holding period, or, equivalently, what fraction of maximum release flux is reached at the beginning of the hold. High remaining fractions are associated with high release flux at the beginning of hold; when this release flux is down to ~20% of the maximum, the remaining fraction of deuterium is only several percent. In contrast, heating to 1275 K – at which temperature release flux is essentially nil – releases virtually all present deuterium.

Combined uncertainties in the QMS calibration and the fraction of D released as unquantifiable molecular species (HDO and D₂O) are found to be small, generally ~20% between different TDS laboratories.

Comparison of desorption spectra demonstrates that instruments with identical heating systems produce essentially identical spectra. It was found that a difference in the positions of desorption peaks can be observed between the instruments with different heating systems (heating plate and oven). This difference has a characteristic appearance, where a system with

a heating plate tends to produce spectra with release peaks at higher temperatures. This behavior was explained by suppression of the heat transfer from the heater to the sample, leading to the actual temperature of a sample being lower than the assumed temperature (i.e., that of the heater). It has been demonstrated that a systematic temperature shift of this type can partially be corrected after the measurement. Following this correction, temperature uncertainty due to sample-specific variations is estimated to be ~60 K. For Be, where release peaks are located in the 800-1000 K range, this translates into an uncertainty in determination of trapping energy of ~15%.

Comparison of TDS and IBA demonstrates that the ratio between deuterium amounts measured by two techniques at different locations across limiter tiles shows a systematic dependence; in the central part of the tile IBA-to-TDS ratio is low, generally below 0.5, and increases towards the periphery, approaching 1. This indicates the difference in retention mechanism between these areas. In the erosion-dominated central part of a tile a large fraction of the deuterium is retained in the bulk, beyond the detection range of IBA; on the other hand, in the deposition-dominated peripheral regions most of the retained deuterium content is retained near the surface, within the reach of IBA. Indeed in the peripheral regions of the tiles, occasionally the IBA-to-TDS ratio exceeds 1, which is unphysical. This can be rationalized by the measurement spots of IBA occasionally containing local areas of increased deuterium content, not reflecting deuterium amount in the sample as a whole, as well as TDS underestimating total retention due to not all D being released during a TDS run.

Comparison of tritium retention values indicate that at low tritium contents – corresponding to those found in JET ILW PFCs at present, $\sim 10^{12}$ - 10^{14} at/cm² (i.e., following only deuterium plasma campaigns) – QMS-based TDS is not suitable for quantification, as opposed to radiometry-based methods such as dissolution. In contrast, at the concentrations of $\sim 10^{16}$ at/cm² QMS-based and radiometry based techniques produce comparable results.

Based on the findings of the study, general recommendations regarding best practices of the TDS measurements can be formulated:

- 1) Maximum temperature in the TDS run should considerably exceed the temperature of the last release peak, such that by the beginning of the maximum temperature holding period the deuterium release flux is considerably lower than at the maximum, ideally at most ~20 % of the maximum value. Otherwise there is a potential for underestimating the values of retention.
- 2) An accurate control and measurement of sample temperature is needed, making the oven-type heating systems preferable to the heating plate-type one, particularly for the thick quarter samples.
- 3) Systems should have the best vacuum that can be achieved to ensure the hydrogen and oxygen background is kept as low as possible, to minimize underestimation of the deuterium content due to release of its fraction in the form of unquantifiable HDO and D₂O molecules, and later tritium containing iso-molecules.

Concerning comparison between different techniques, general observations can be made as well:

- 1) TDS and IBA yield comparable results in terms of deuterium retention. The differences in retention values that are observed in Be samples from JET ILW limiter tiles are due to the different retention mechanisms in different regions of the tiles.

- 2) TDS and dissolution yield comparable results in terms of tritium retention – with an important caveat that this is the case when tritium concentration is sufficiently high, above $\sim 10^{14}$ - 10^{16} atoms/cm². At lower tritium concentrations the tritium signal is below the limit of detection due to the intrinsic noise level, so QMS-based determination of tritium content is impossible. Radiometric techniques, such as dissolution of radiometry-based TDS, are preferable (indeed they present the only possibility) for measurements of tritium retention in these conditions (which, incidentally, characterize current tritium contents in ILW JET PFCs).

Overall it should be emphasized that even though discrepancies were observed between different TDS facilities on one hand, and between TDS and other techniques, these measurements can still provide valuable fuel quantification and trapping energy data. Even in the worst cases discrepancy in retention of inhomogeneous samples and T between different TDS facilities is $\sim 250\%$ (a factor of 3.5). For rather homogeneously prepared D and H reference samples a factor of 1.4 was determined between different TDS facilities. Comparison between different techniques show that when their ranges of applicability overlap (i.e., comparing TDS and radiometry-based dissolution – when tritium amount is sufficiently high; comparison TDS and IBA – when deuterium is concentrated close to the surface within the probing range of IBA), their results are comparable as well.

Acknowledgements

This work has been carried out within the framework of the EUROfusion Consortium, funded by the European Union via the Euratom Research and Training Programme (Grant Agreement No 101052200 — EUROfusion). Views and opinions expressed are however those of the author(s) only and do not necessarily reflect those of the European Union or the European Commission. Neither the European Union nor the European Commission can be held responsible for them.

This work has been part-funded by the EPSRC Energy Programme (grant number EP/W006839/1). To obtain further information on the data and models underlying this paper please contact PublicationsManager@ukaea.uk.

The research used UKAEA's Materials Research Facility, which has been funded by and is part of the UK's National Nuclear User Facility and Henry Royce Institute for Advanced Materials.

The work has been supported by the Swedish Research Council (VR), Grant 2015–04844. Financial support of the Tandem Accelerator Infrastructure by VR-RFI (contract #2017-00646_9) as well as the Swedish Foundation for Strategic Research (SSF) under contract RIF14-005 is gratefully acknowledged.

References

- [Federici2001] G. Federici et al., Nucl. Fusion 41 (2001) 1967.
[Counsell2] G.C. Counsell et al., Plasma Phys. Control Fusion 48 (2006) B189.
[Loarte2007] A. Loarte et al., Nucl. Fusion 47 (2007) S203 (ITER Physics Basis, Chapter 4).

- [Rohde2001] V. Rohde et al., J. Nucl. Mater. 290-293 (2001) 317.
- [Whyte1999] D. Whyte et al., Nucl. Fusion 39 (1999) 1025.
- [Rubel1989] M. Rubel et al., J. Nucl. Mater. 161 (1989) 153.
- [Mayer2001] M. Mayer et al., J. Nucl. Mater. 290-293 (2001) 381.
- [Rubel2001] M. Rubel, P. Wienhold, D. Hildebrandt, J. Nucl. Mater. 290-293 (2001) 473.
- [Skinner1977] C.H. Skinner et al., J. Nucl. Mater 241-243 (1977) 214.
- [Mueller1977] D. Mueller et al., J. Nucl. Mater 241-243 (1977) 897.
- [Coad1989] J.P. Coad et al., J. Nucl. Mater. 162-164 (1989) 533.
- [Coad1997] J.P. Coad et al., J. Nucl. Mater. 241-243 (1997) 408.
- [Coad2001] J.P. Coad et al., J. Nucl. Mater. 290-293 (2001) 224.
- [Andrew1999] P. Andrew et al., Fusion Eng. Design 47 (1999) 233.
- [Coad2018] J.P. Coad et al., Fusion Eng. Design 138 (2018) 78.
- [Penzhorn2001] R-D. Penzhorn et al., J. Nucl. Mater. 288 (2001) 170.
- [Rubel2003] M. Rubel et al., J. Nucl. Mater. 313-316 (2003) 321.
- [Rubel2012] M. Rubel et al., Fusion Eng. Design 87 (2012) 935.
- [Matthews2007] G.F. Matthews et al., Phys. Scr. T128 (2007) 137.
- [Matthews2011] G.F. Matthews et al., Phys. Scr. T145 (2011) 014001.
- [Matthews2013] G.F. Matthews J. Nucl. Mater. 438 (2013) S2.
- [Loarer2013] T. Loarer et al., J. Nucl. Mater 438 (2013) S108.
- [Brezinsek2013] S. Brezinsek et al., J. Nucl. Mater 438 (2013) S303.
- [Loarer2007] T. Loarer et al., Nucl. Fusion 47 (2007) 1112.
- [Tsitrone2011] E. Tsitrone et al., J. Nucl. Mater. 415 (2011) S735.
- [Pegourie2013] B. Pégourié et al., J. Nucl. Mater. 438 (2013) S120.
- [Rubel2007] M. Rubel et al., J. Nucl. Mater. 363-365 (2007) 877.
- [Rebut1985] H. Rebut et al., Nucl. Fusion 25 (1985) 1011.
- [Coad1991] J.P. Coad et al., J. Nucl. Mater. 176-177 (1991) 145.
- [Petersson2011] P. Petersson et al., Phys. Scr. T145 (2011) 014014.
- [Petersson2012] P. Petersson et al., Nucl. Instrum. Meth. B 273 (2012) 113.
- [Bykov2015] I. Bykov et al., Nucl. Instrum. Meth. B 342 (2015) 19.
- [Gibney2022] Gibney, E. (2022). Nuclear-fusion reactor smashes energy record. Nature, 602(7897), 371. <https://doi.org/10.1038/D41586-022-00391-1>
- [Mass1999] A.C. Mass et al., Fusion Eng. Design 47 (1999) 247.
- [Hillis1997] D.L. Hillis et al., Fusion Eng. Design 34-35 (1997) 347.
- [Lasser1999] R. Lässer et al., Fusion Eng. Design 47 (1999) 173.
- [Lasser1999-2] R. Lässer et al., Fusion Eng. Design 47 (1999) 333.
- [Summers2001] D.D.D. Summers et al., J. Nucl. Mater 290-293 (2001) 496
- [Huber2001] A. Huber et al., Phys. Scr. T94 (2001) 102.
- [Schweer2007] B. Schweer et al., J. Nucl. Mater 363-365 (2007) 1375.
- [Gierse2011] N.Gierse, B.Schweer, A.Huber, O.Karger, V.Philipps, U.Samm, G.Sergienko, Journal of Nuclear Materials 415 (2011) S1195-S1198
- [Grisolia2007] Grisolia, C., Semerok, A., Weulersse, J. M., le Guern, F., Fomichev, S., Brygo, F., Fichet, P., Thro, P. Y., Coad, P., Bekris, N., Stamp, M., Rosanvallon, S., & Piazza, G. (2007). In-situ tokamak laser applications for detritiation and co-deposited layers studies,

- Journal of Nuclear Materials*, 363–365(1–3), 1138–1147.
<https://doi.org/10.1016/j.jnucmat.2007.01.169>.
- [Semerok2016] Semerok, A., L’Hermite, D., Weulersse, J. M., Lacour, J. L., Cheymol, G., Kempenaars, M., Bekris, N., & Grisolia, C. (2016). Laser induced breakdown spectroscopy application in joint European torus. *Spectrochimica Acta - Part B Atomic Spectroscopy*, 123, 121–128. <https://doi.org/10.1016/j.sab.2016.08.007>.
- [Philipps2013] V. Philipps et al., *Nucl. Fusion* 53 (2013) 093002.
- [Malaquias2013] A. Malaquias et al., *J. Nucl. Mater.* 438 (2013) S936.
- [Zlobinski2020] M. Zlobinski et al., *Phys. Scr.* T171 (2020) 014075
- [Hartwig2015] Z.S. Hartwig et al., “Fuel retention measurements in Alcator C-Mod using accelerator-based in situ materials surveillance” *J. Nucl. Mater.* 463 (2015) 73.
- [Widdowson2007] A. Widdowson et al., *J. Nucl. Mater.* 363-365 (2007) 341.
- [Likonen2019] J. Likonen et al., *Nucl. Mater. Energy* 19 (2019) 300.
- [Baron2015] A. Baron-Wiechec et al., *J. Nucl. Mater.* 463 (2015) 157.
- [Petersson2015] P. Petersson et al., *J. Nucl. Mater.* 463 (2015) 814.
- [Heinola2016] K. Heinola et al., *Phys. Scr.* T167 (2016) 014075.
- [Heinola2017] K. Heinola et al., *Nucl. Fusion* 57 (2017) 086024.
- [Heinola2017-2] K. Heinola et al., *Phys. Scr.* T170 (2017) 014063.
- [Widdowson2017] A. Widdowson et al., *Nucl. Mater. Energy* 12 (2017) 499.
- [Widdowson2017-2] A. Widdowson et al., *Nuclear Fusion* 57 (2017) 086045.
- [Widdowson2020] A. Widdowson et al., *Phys. Scr.* T171 (2020) 014051.
- [Krat2020] S. Krat et al., *Phys. Scr.* T171 (2020) 014059.
- [Mayer2016] M. Mayer et al., *Phys. Scr.* T167 (2016) 014051.
- [Rubel2017] M. Rubel et al., *Nucl. Fusion* 57 (2017) 066027.
- [Rubel2016] M. Rubel et al., *Nucl. Instrum. Meth.* B371 (2016) 4.
- [Catarino2017] N. Catarino, N. P. Barradas, V. Corregidor, A. Widdowson, A. Baron-Wiechec, J. P. Coad, K. Heinola, M. Rubel, E. Alves, and JET contributors, *Nuclear Materials and Energy* 12 (2017) 559-563.
- [Rubel2020] M. Mayer et al., *Nucl. Fusion* 60 (2020) 025001.
- [Mayer2009] M. Mayer et al., *Nucl. Mater. Meth. B* 267 (2009) 506.
- [Bykov2012] I. Bykov et al., *Nucl. Instrum. Meth. B* 273 (2012) 250.
- [Kubota2006] N. Kubota et al., “Surface Analysis for TFTR armour tile exposed to D-T plasmas using nuclear technique”, 21th IAEA Conf on Fusion Energy, 2006, EX/P4-12, https://www-pub.iaea.org/MTCD/Meetings/FEC2006/ex_p4-12.pdf
- [Strom2016] P. Ström et al., *Rev. Sci. Instrum.* 87 (2016) 103303.
- [Strom2019] P. Ström et al., *J. Nucl. Mater.* 516 (2019) 202.
- [Friedrich2001] M. Friedrich et al., *Phys. Scr.* T94 (2001) 98.
- [Ruset2016] C. Ruset et al., *Phys. Scr.* T167 (2016) 014049.
- [Likonen2003] J. Likonen et al., *Fusion Eng. Design* 66-68 (2003) 219
- [Coad2018] J.P. Coad et al., *Fusion Eng. Design* 138 (2018)
- [Zlobinski2019] Zlobinski, M., Sergienko, G., Martynova, Y., Matveev, D., Unterberg, B., Brezinsek, S., Spilker, B., Nicolai, D., Rasinski, M., Möller, S., Linsmeier, C., Lungu, C. P., Porosnicu, C., Dinca, P., & de Temmerman, G. (2019). Laser-Induced Desorption of

- co-deposited Deuterium in Beryllium Layers on Tungsten. *Nuclear Materials and Energy*, 19, 503–509. <https://doi.org/10.1016/j.nme.2019.04.007>.
- [Hatano2015] Y. Hatano et al., *J. Nucl. Mater.* 463 (2015) S966.
- [Hatano2016] Y. Hatano et al., *Phys. Scr.* T167 (2016) 014009.
- [Lee2020] S. Lee, Y. Hatano et al., *Fusion Eng. Design* 160 (2020) 111959.
- [Lee2021] S. Lee, Y. Hatano et al., *Nucl. Mater. Energy* 26 (2021) 100930.
- [Otsuka2018] T. Otsuka et al., *Nucl. Mater. Energy* 17 (2018) 279.
- [Hatano2017] Y. Hatano et al., *Phys. Scr.* T170 (2017) 014014.
- [Pajuste2017-2] Pajuste, E., Kizane, G., Vitins, A., Igaune, I., Avotina, L., Zarins, R., & JET Contributors. (2017). Structure, tritium depth profile and desorption from ‘plasma-facing’ beryllium materials of ITER-Like-Wall at JET. *Nuclear Materials and Energy*, 12, 642–647. <https://doi.org/10.1016/j.nme.2017.03.017>.
- [Ashikawa2020] N. Ashikawa et al., *Nucl. Mater. Energy* 22 (2020) 100673.
- [Pajuste2017] E. Pajuste et al., *Nucl. Fusion* 57 (2017) 102001.
- [Ziegler1996] J.F. Ziegler et al., *The Stopping and Range of Ions in Solids*, second edition, Pergamon, New York, 1996.
- [Zlobinski2019] M. Zlobinski et al., *Fusion Engineering and Design* 146 (2019) 1176–1180.
- [Xiao2013] Q.Xiao, A.Huber, G.Sergienko, B.Schweer, Ph.Mertens, A.Kubina, V.Philipps, H.Ding, *Fusion Engineering and Design* 88 (2013) 1813-1817.
- [Oelman2018] J.Oelmann, N.Gierse, C.Lia, S.Brezinsek, M.Zlobinski, B.Turan, S.Haas, Ch.Linsmeier, *Spectrochimica Acta Part B: Atomic Spectroscopy* 144 (2018) 38-45.
- [Baron2018] A. Baron-Wiechec, K. Heinola, J. Likonen, E. Alves, N. Catarino, J. P. Coad, V. Corregidor, I. Jepu, G. F. Matthews, A. Widdowson, JET Contributors, *Thermal desorption spectrometry of beryllium plasma facing tiles exposed in the JET tokamak*, *Fusion Engineering and Design* 133 (2018) 135-141.
- [Catarino2020] N Catarino , A Widdowson , A Baron-Wiechec , J P Coad, K Heinola , M Rubel , N P Barradas , E Alves and JET Contributors, *Phys. Scr.* T171 (2020) 014044.
- [Pajuste2019] Pajuste, E., Kizane, G., Avotina, L., Teimane, A. S., Lescinskis, A., & Vonda, K., *Nuclear Fusion* 59 (2019) 10.
- [Matei2008] Matei L., Postolache C., Bubueanu G., Podina C, *Synthesis of Labeled Compounds using Recovered Tritium from Expired Beta Light Sources*, *Fusion Sci Technol*, 54 (2008) 643, DOI: [10.13182/FST08-A1897](https://doi.org/10.13182/FST08-A1897)
- [Raty2019] A.Raty, et al.(2019), Characterization measurements of fluental and graphite in FiR1 TRIGA research reactor decommissioning waste, *Nucl. Eng. Des.*, 353, (2019), 110198, DOI:10.1016/j.nucengdes.2019.110198
- [Fugaru2020] V. Fugaru, G. Bubueanu, C. S. Tuta, M-R. Ioan, *Radiological Characterization of the Resulting Solid Materials from the Refurbishment of the Tritium Laboratory*, *Fusion Sci Technol*, 76, 3 (2020), 347, [dx.doi.org/10.1080/15361055.2020.1712008](https://doi.org/10.1080/15361055.2020.1712008)
- [Dinca2021] P. Dinca, C. Staicu, C. Porosnicu, O. G. Pompilian, A. M. Banici, B. Butoi, C. Lungu, I. Burducea, *Coatings* 11 (2021) 1430
- [Pajuste2021] E Pajuste^{1,2} , A S Teimane¹ , G Kizane¹ , L Avotina¹ , M Halitovs¹ , A Lescinskis¹ , A Vitins¹ , P Kalnina¹ , E Lagzdina¹ , R J Zablockis¹ JET Contributors^{3,4}, *Phys. Scr.* 96 (2021) 124050.

Table 1 Analysis of hydrogen isotopes in controlled fusion devices with emphasis on JET (List limited to methods used in fuel retention studies)

	Technique	Advantages	Disadvantages/ Limitations	Remark/ Reference
In-situ	Optical spectroscopy	H/D ratio		[Hillis1997][Lasser1999]
	Gas input/feed	Direct measurement of gas flow and pressure.		Essential to prepare and sustain discharges.
	Gas balance by QMS	Direct measurements: shot-by-shot or after operation day		Common in most machines [Mayer2001][Loarer2007][Tsitrone2011][Pegourie2013]
	Radiometry: beta and gamma	(a) Assessment of T from D-D reaction (b) Activation by D-D and D-T neutrons	Low accuracy. Limited to PFC surface in areas accessible by RH.	Possible only during shut-down period
	AIMS	Inter-shot study.	Limited to small and medium-size machines without permanent magnetic field	Only early tests performed in Alcator C-Mod [Hartwig2015]
	Calorimetry	Precise determination of T inventory in the storage bed.		[Lasser1999][Lasser1999-2]
	LIAS	Spatial analysis		JET [Summers2001] TEXTOR [Huber2001][Schweeer2007][Gierse2011]
	LID – QMS	Spatial analysis Inter-shot analysis		TEXTOR [Huber2001] Under development for ITER. Test in JET under preparation.
	LIBS	Spatial analysis		Tested in laboratory. Limited in-situ experiments on JET

			[Grisolia2007][Semerok2016]. Proposal for remote handling system for deployment during in-vessel maintenance.	
Ex-situ	TDS – flash/fast temperature rump.	Fast qualitative assessment of H isotopes in PFC.	Need of cross-calibration.	Process occurs also in-situ from PFC under high heat load/transient events. Flash lamp tested on JET tiles for fuel removal, but the isotope release was not directly monitored [Widdowson2007]
	TDS – steady temperature ramp	Determination of binding states. Total inventory if combined with outgassing at maximum temperature.	Need of a calibration using calibrated leak. Temperature limited to 1273 K in most systems.	Temperature limited to 1073 K for Be samples (evaporation) [Likonen2019].
	NRA for H $p(^{15}\text{N},\alpha)^{12}\text{C}$	Selective for H.	Expensive ^{15}N . Information depth limited $< 1 \mu\text{m}$.	Not done on JET materials.
	NRA for D $\text{D}(^3\text{He},\alpha)^4\text{He}$	Quantification and depth profiling down to $20 \mu\text{m}$ in low-Z substrates.	Expensive ^3He . Overlap of C and Be peaks make low concentrations hard to deconvolve.	Most important and always used method for PFC analysis [Baron2015][Pettersson2015][Heinola2016][Heinola2017][Heinola2017-2][Widdowson2017][Widdowson2017-2][Widdowson2020][Krat2020][Mayer2016][Rubel2017][Rubel2016][Rubel202

			0]. Simultaneous analysis of C, Be but the information depth is too small for thick co-deposits even with a 6 MeV beam [Mayer2009].
NRA for T $T(^{12}\text{C},\alpha)^{11}\text{B}$ $T(^{12}\text{C},p)^{14}\text{C}$ $T(d,\alpha)n$		Low sensitivity of ^{12}C -t reactions Neutron generation in d-t reaction.	Both ^{12}C -t reactions tried on JET materials [Bykov2012], while the d-t reaction was used on TFTR tiles [Kubota2006]
ERDA	Quantitative depth profiling of all isotopes.	Information depth < 1 μm	[Pettersson2012] [Baron2015][Strom2016][Strom2019]
AMS	Depth profiling of all H isotopes.	Difficult sample preparation.	[Friedrich2001]
GDOES	Detection and depth profiling of all H isotopes. Large information (sputter) depth possible up to 100 μm [Ruset2016].	Problems with calibration for D.	[Ruset2016]
SIMS	Detection and depth profiling of all H isotopes and He. Isotopic ratio at a given depth. Large information (sputter) depth possible.	Challenging quantification in mixed materials. Sensitivity depends on chemical surrounding/material composition.	[Likonen2019][Likonen2003][Coad2018]
LIAS			Under development. Not tested in vessel during JET shutdown.

	LIDS & LID-QMS	Rapid desorption	Need of calibration using calibrated leak. Risk of desorption from the spot-adjacent region	[Zlobinksi2019]
	LIBS			[Xiao2013] [Oelman2018]
Ex-situ for tritium	Off-gassing			T analysis: isotopic exchange of released T in water vapour. Dissolution of HTO in water bubbler and analysis by LSC.
	Radiography (IPT)	T distribution map in the surface and subsurface layer up to 4 μm dependent on the substrate and co-deposit composition. In combination EPMA/EDX T determination in individual elements.	Limited and substrate dependent information depth. No quantification.	[Hatano2015][Hatano2016][Lee2020][Lee2021][Otsuka2018]
	BIXS	T distribution map in the surface and subsurface layer up to 4 μm dependent on the substrate and co-deposit composition. Information on other species based on X-ray spectrum		[Hatano2017]
	TDS		QMS systems have relatively high limit of detection level compared with radio-metric detection methods.	T analysis by LSC [Ashikava2020]. T analysis by proportional counter [Pajuste2017-2]. T analysis by QMS discussed in this work.

Full combustion			T analysis by LSC [Ashikava2020]
Dissolution			T analysis by LSC [Pajuste2017]

Table 2 Composition of the surface region of the tungsten coatings in atomic concentrations (at %) of elements

	Concentration, at. %
W	76.1
D	1.6
H	0.4
C	1.1
N	5.4
O	13.4
Ar	1.2

Table 3 D retention in reference samples

IBA IST, D/cm ²	IBA UU, D/cm ²	TDS A, D/cm ²	TDS B Sample 1, D/cm ²	TDS B Sample 2, D/cm ²	TDS D, D/cm ²
7.4×10^{17}	8.8×10^{17}	1.1×10^{18}	8.2×10^{17}	7.9×10^{17}	8.8×10^{17}

Table 4 T retention in tritiated samples

TDS A	TDS B	Dissolution C
$5.75 \cdot 10^{15}$	$1.85 \cdot 10^{16}$	$1.36 \cdot 10^{16}$

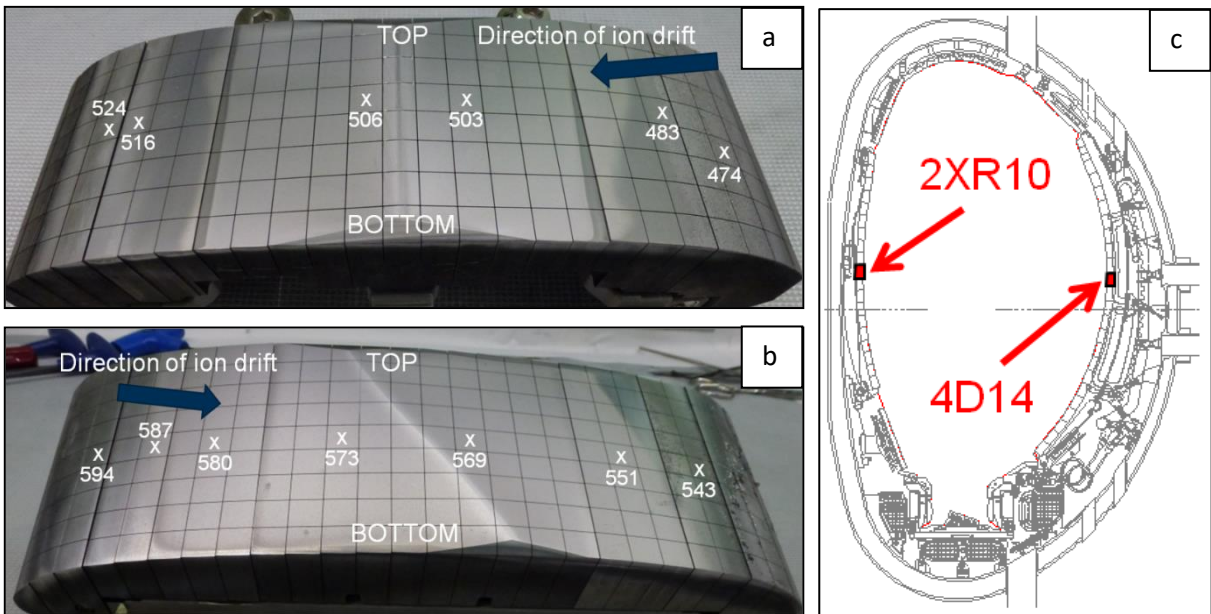


Fig. 1 Images of Be tiles where quarter samples were cut, crosses indicate individual castellations that were used for producing them (a) inner wall guard limiter tile 2XR10; (b) wide poloidal limiter tile 4D14; (c) poloidal locations of these tiles.

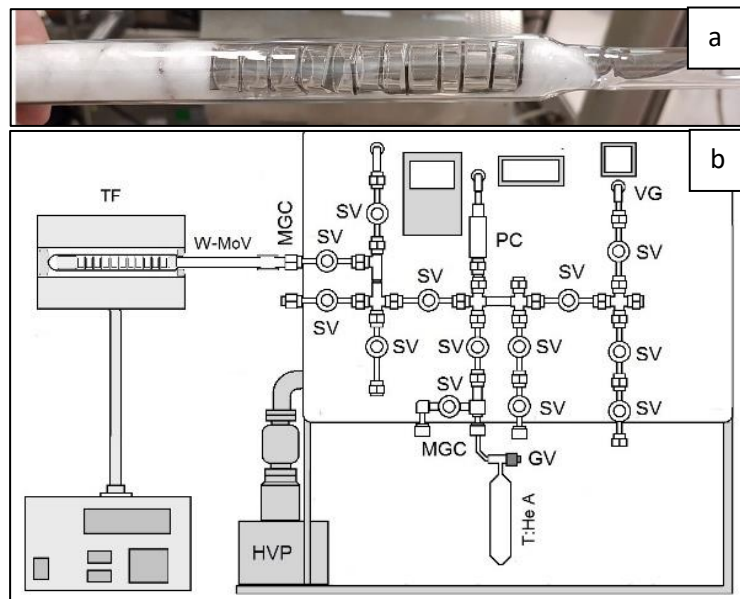


Fig. 2 (a) The glass vials with W-Mo samples; Facility for tritiation of W-Mo samples: TF- Tubular furnace, glass vials with W-Mo samples, MGC- Metal-glass connectors, HVP – High vacuum pump, SV- Swagelok valves, GV- Glass valves, PC- Pressure controller, VG- Vacuum gauge, T:He A- $T_2\cdot^3\text{He}$ ampule

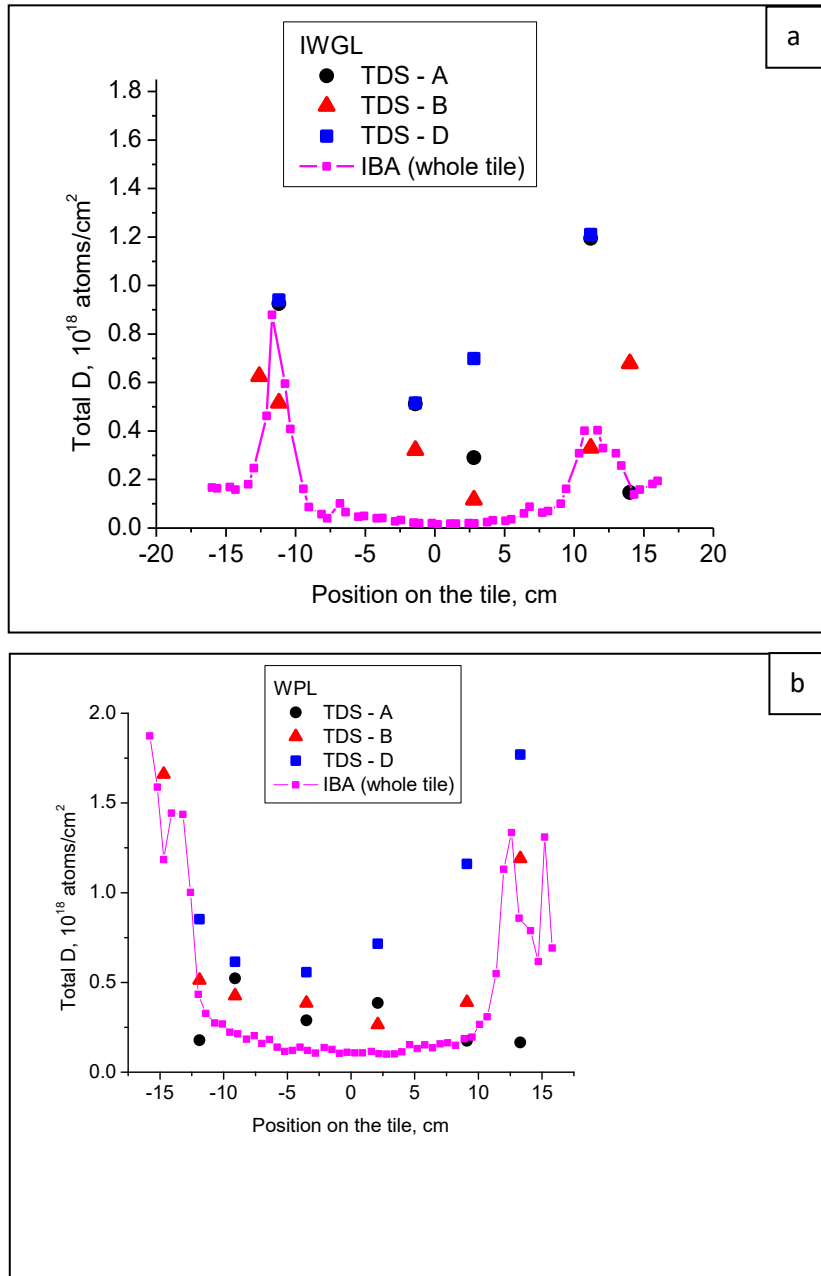


Fig. 4 Comparison of the TDS results from quarter samples and corresponding IBA line scans: (a) IWGL tile; (b) WPL tile.

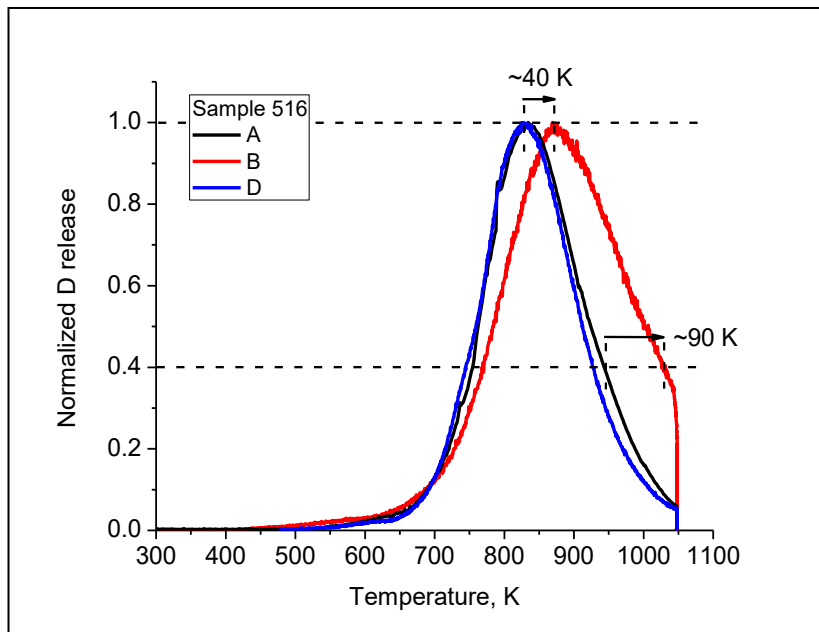


Fig. 5 Comparison of the normalized D desorption spectra from a set of quarter samples measured at different facilities.

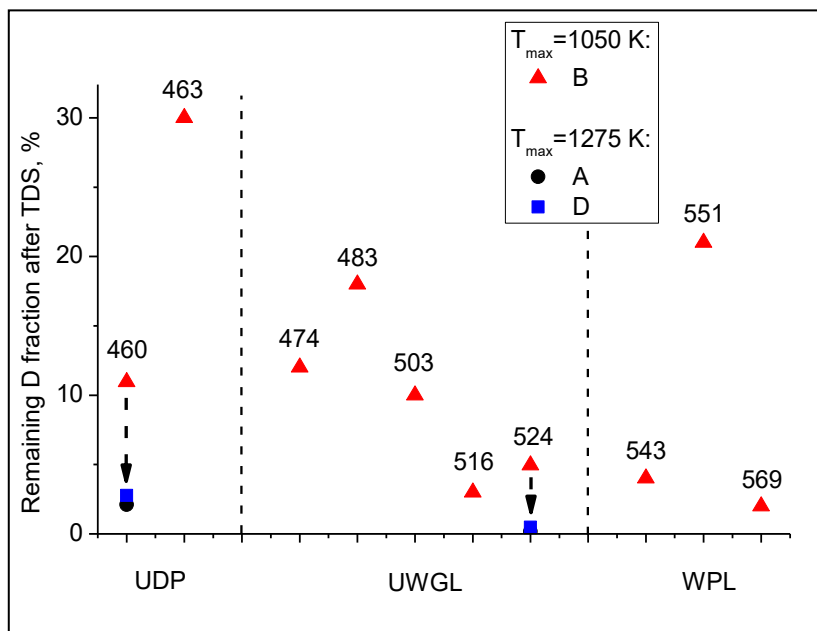


Fig. 6 Remaining percentage of D measured by IBA after a TDS run relative to that measured by IBA before a TDS run, for specified samples.

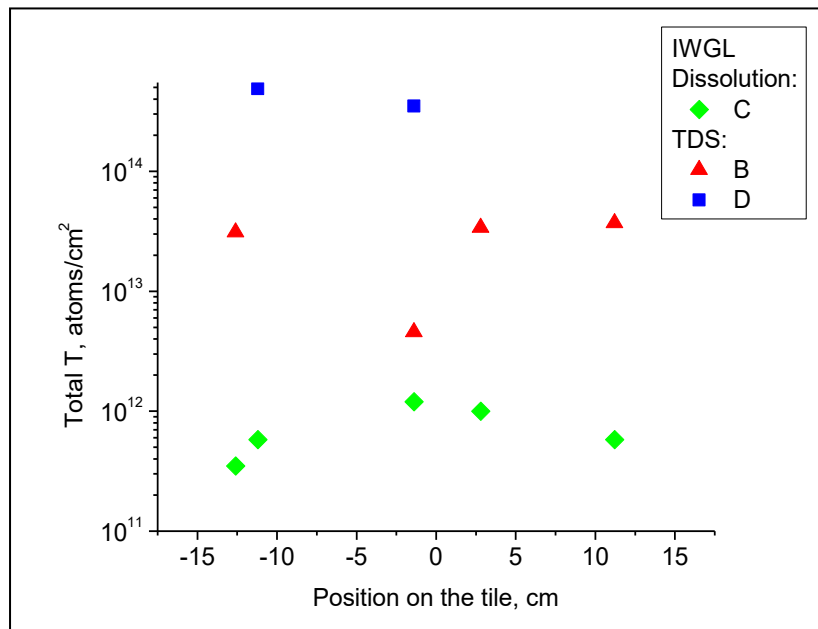


Fig. 7 Comparison of tritium amounts measured by TDS at different facilities and by dissolution.

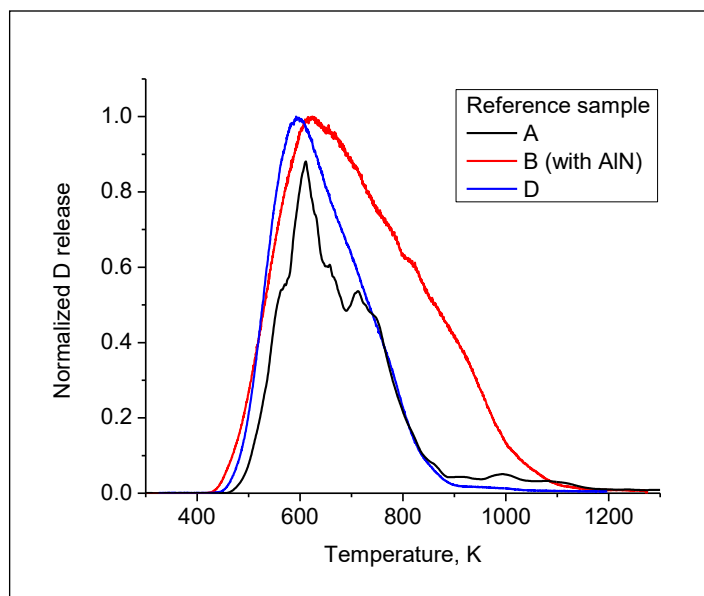


Fig. 8 Comparison of the D desorption spectra obtained from reference samples at different facilities.

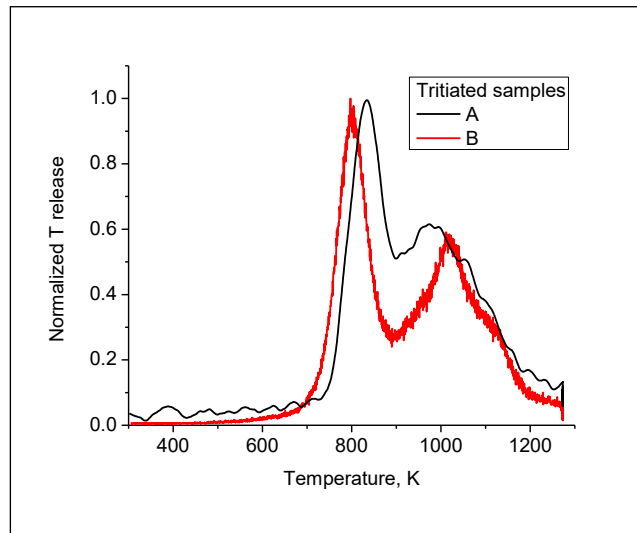


Fig. 9 Comparison of the T desorption spectra obtained from reference samples at different facilities

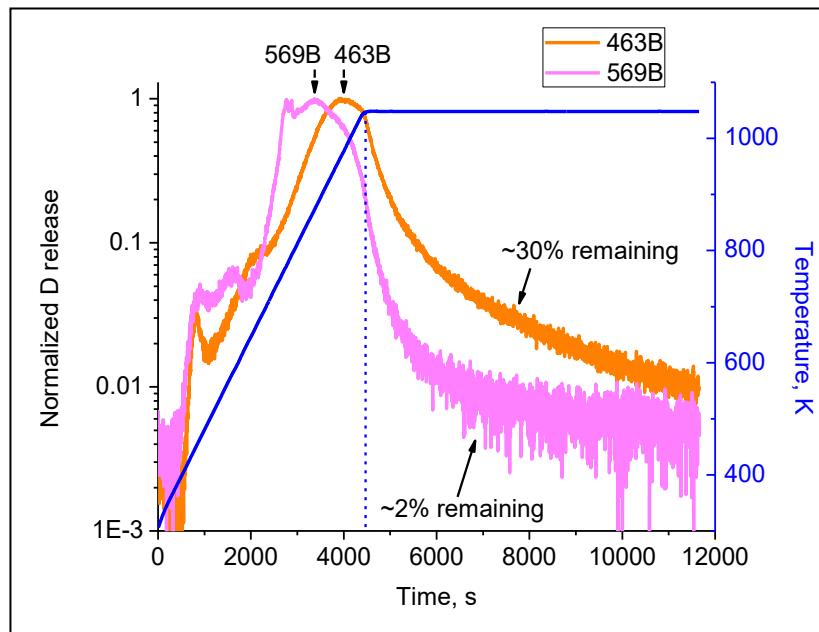


Fig. 10 Comparison of the normalized D spectra obtained at facility B using two samples with significantly different percentages of D remaining after a TDS run.

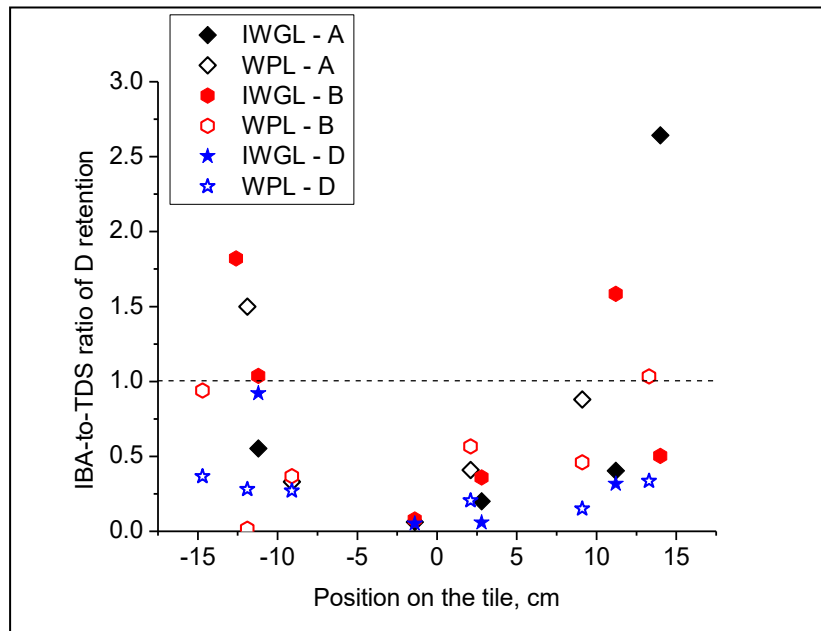


Fig. 11 Comparison of the ratios of D amounts measured by IBA and TDS for different quarter samples across IWGL and WPL tiles.

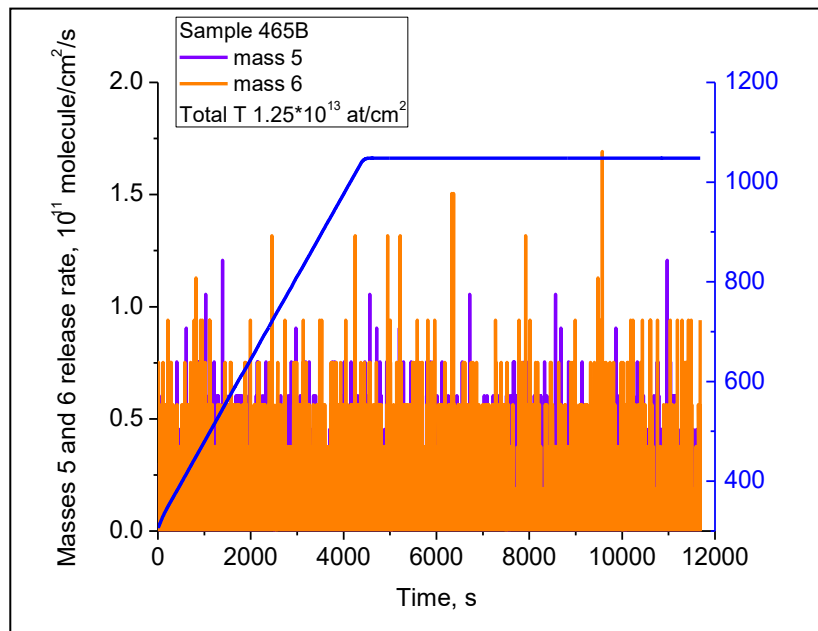


Fig. 12 Typical desorption spectra of masses 5 and 6 measured in facility B.

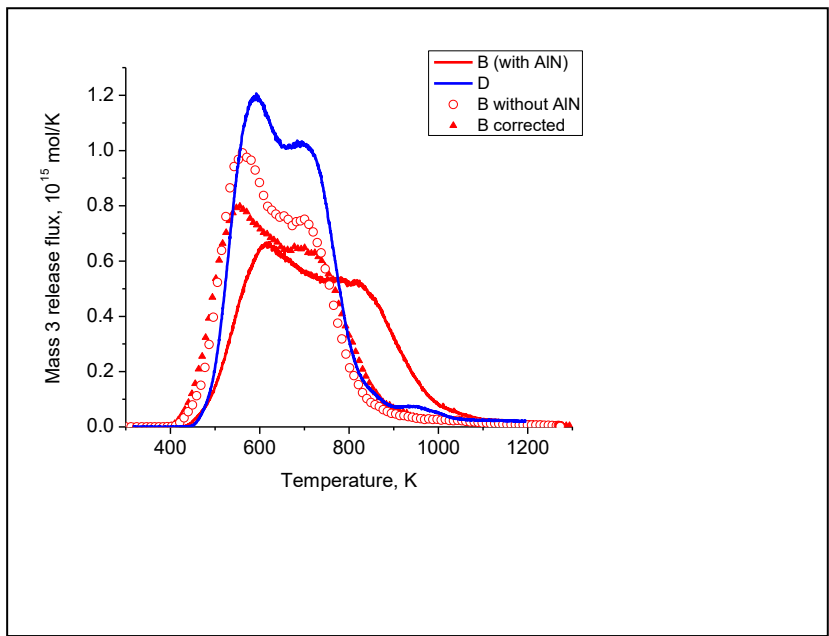


Fig. 13 TDS spectra obtained on reference samples at different facilities, and in facility B without protective AlN layer.

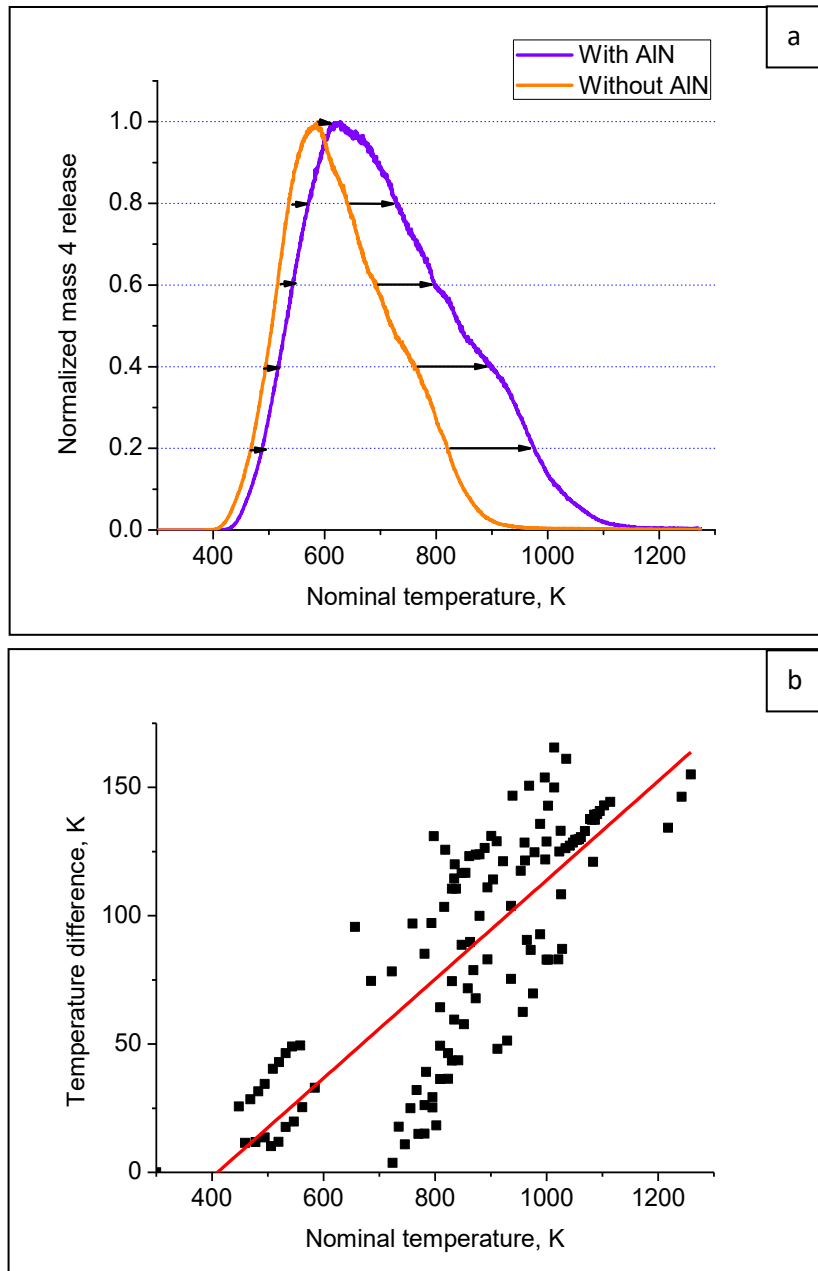


Fig. 14 (a) Comparison of the normalized mass 4 release spectra obtained from the reference samples at facility B, with and without ALN protective layer, illustrating the temperature shift introduced by ALN; (b) dependence of temperature shift introduced by ALN on nominal heater temperature.

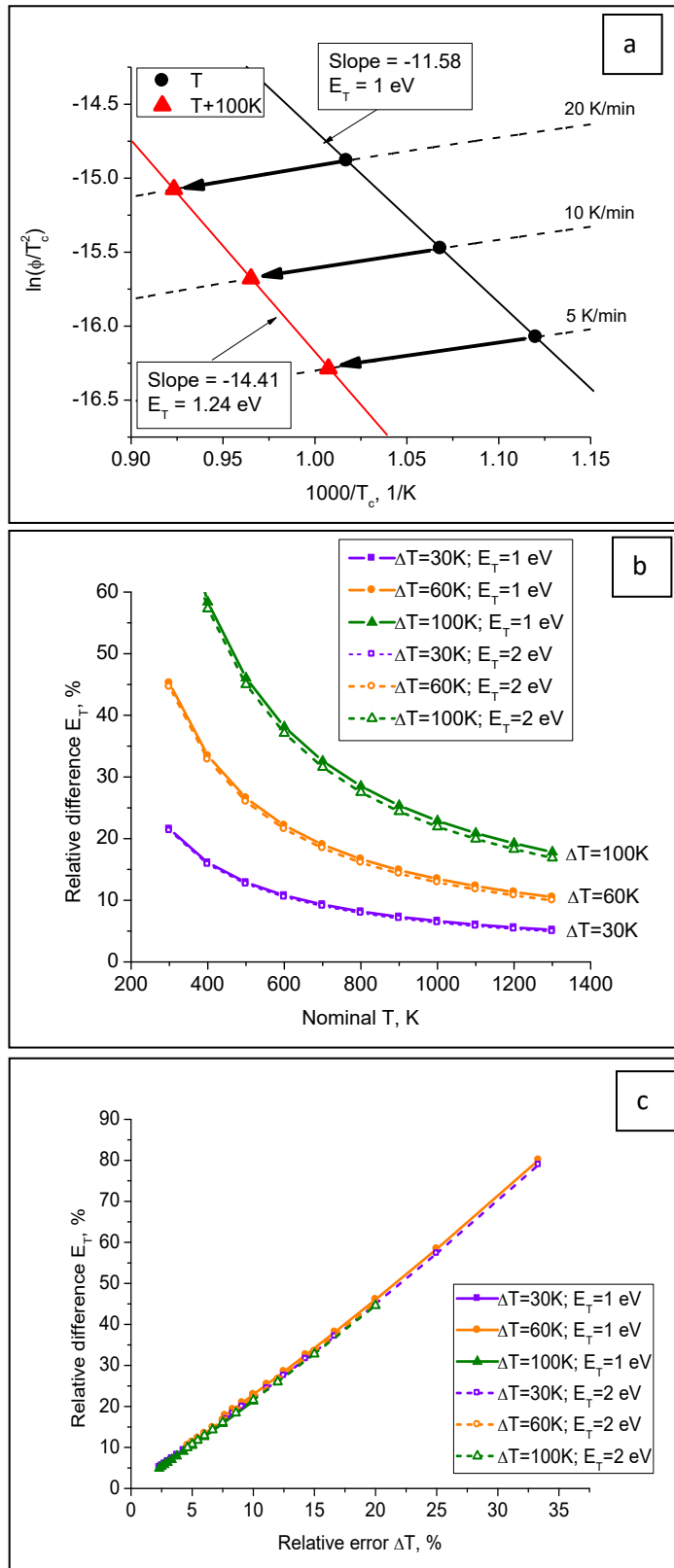


Fig. 15 (a) An example of the simulated shift of peak positions caused by the temperature uncertainty of 100 K for heating rates of 5, 10 and 20 K/min; (b) dependence of relative uncertainty of E_T corresponding to the temperature uncertainties of 30, 60 and 100 K as a function of nominal temperature; (c) dependence of relative uncertainty of E_T as a function of relative temperature uncertainty.